Kinetic models for wave propagation in random media
Application to Time Reversal

Guillaume Bal

Department of Applied Physics & Applied Mathematics

Columbia University

http://www.columbia.edu/∼gb2030

gb2030@columbia.edu

Outline

1. Time Reversal in random media and kinetic models

2. Statistical stability and rigorous theories

3. Validity of Radiative Transfer Models

4. Applications to Detection and Imaging

Time Reversal framework

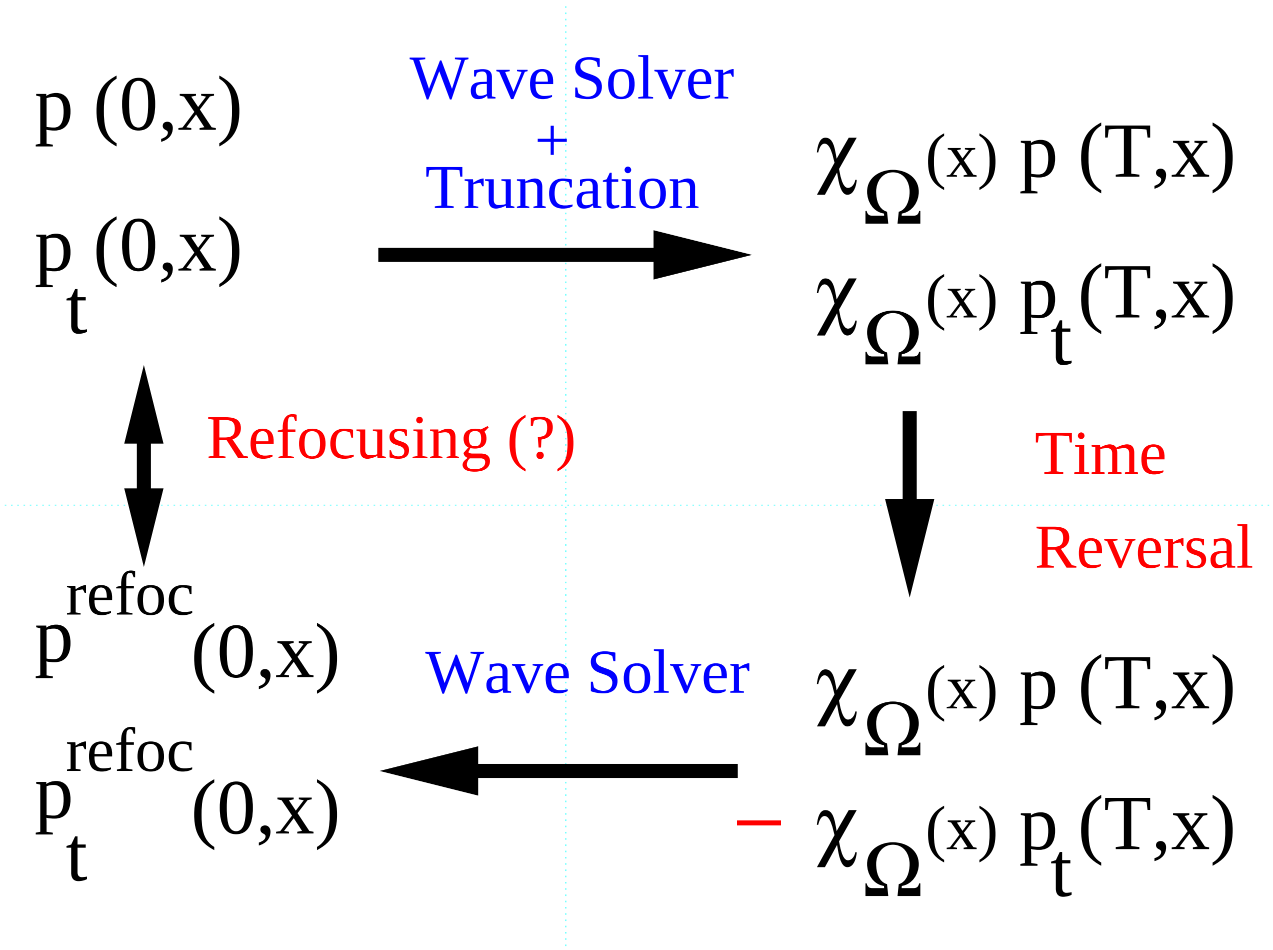

Numerical Experiment: Initial Data

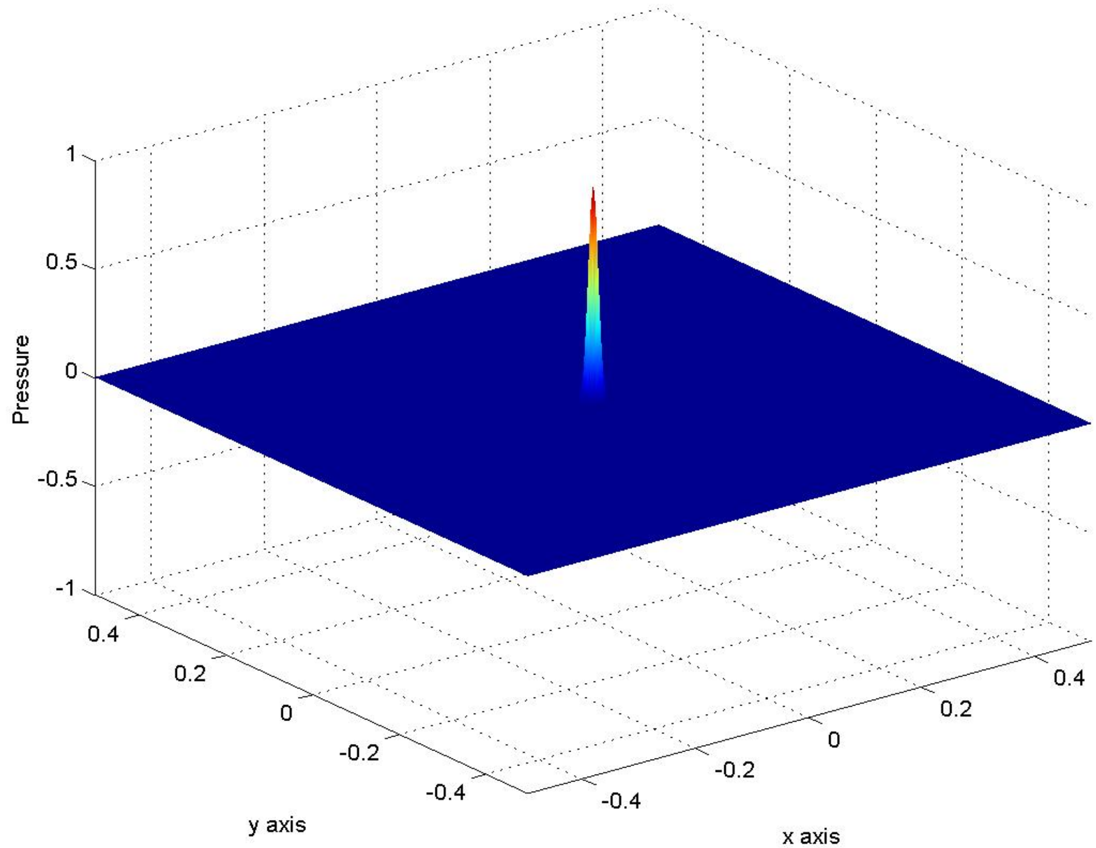

Numerical Experiment: Forward Solution

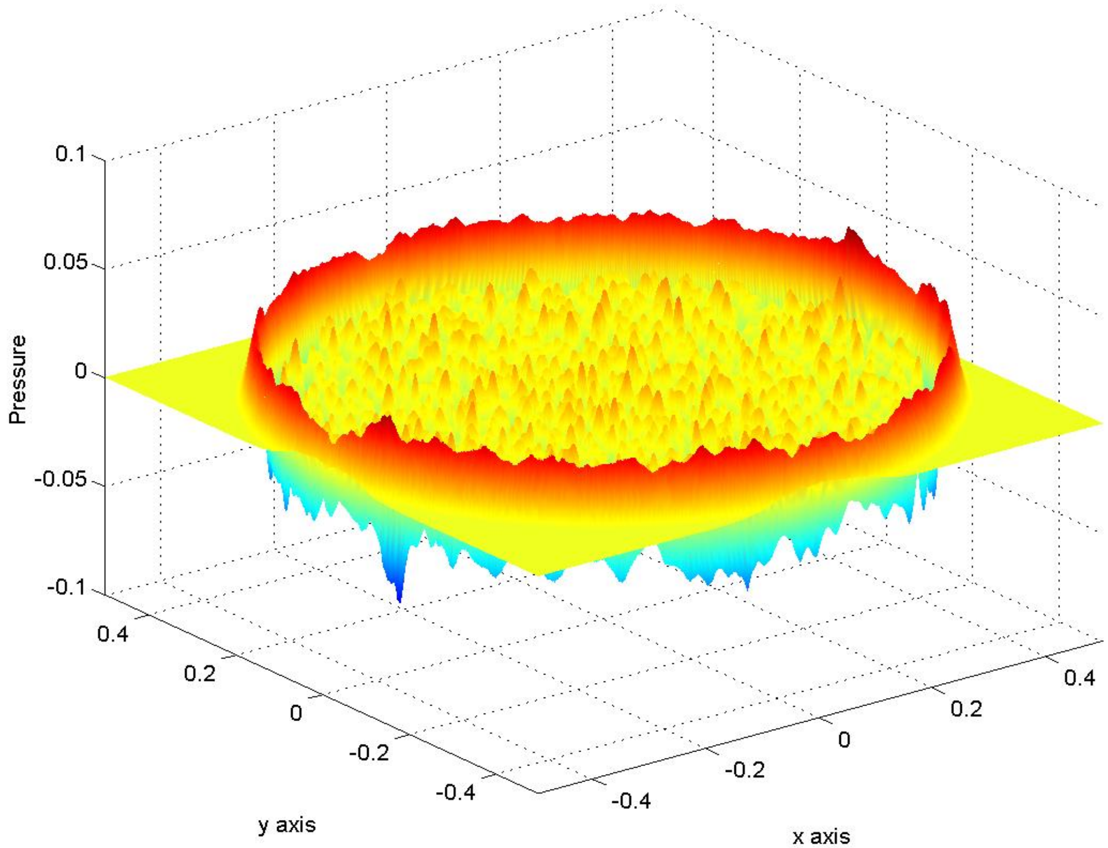

Numerical Experiment: Truncated Solution

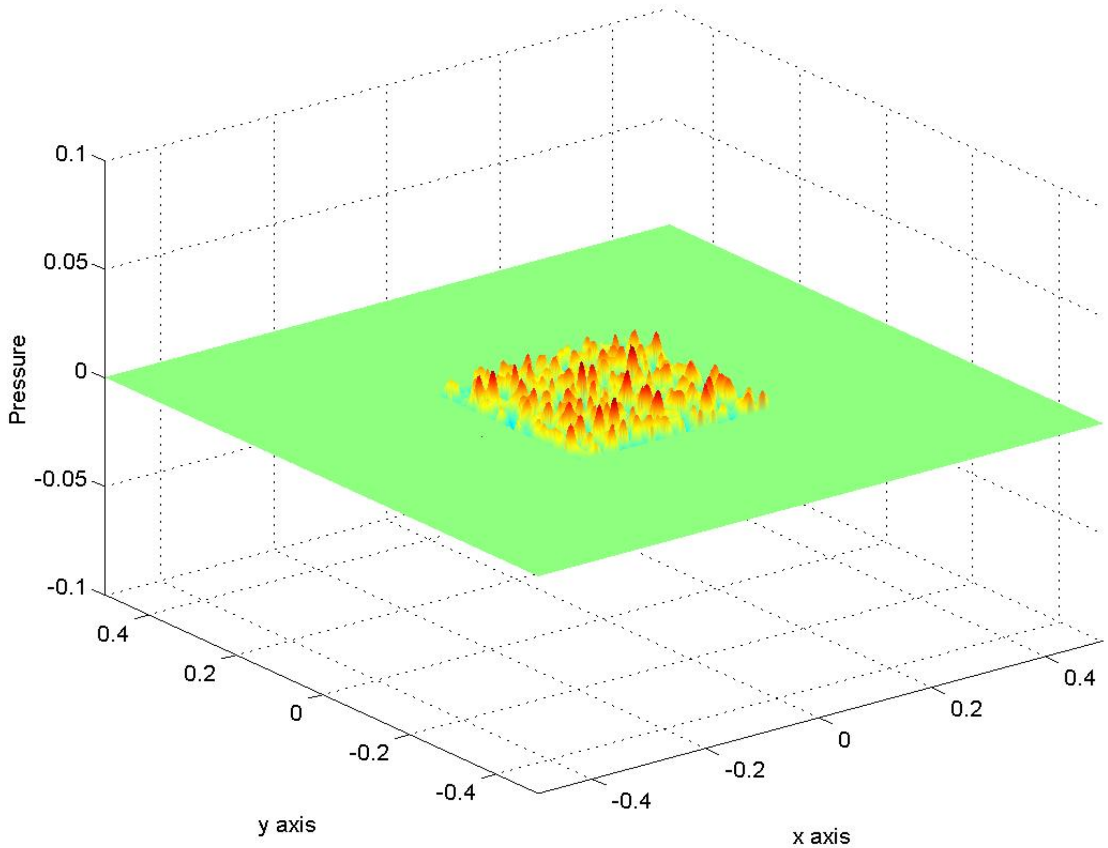

Numerics: Time-reversed Solution

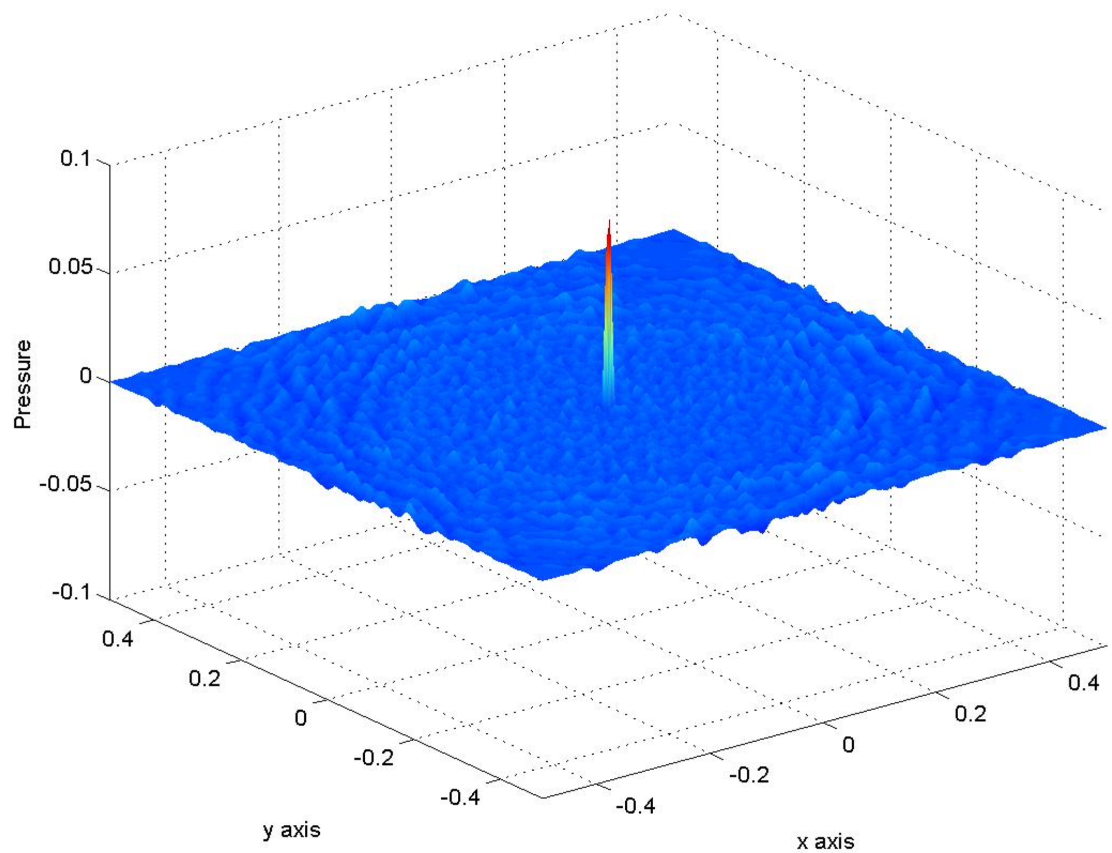

Numerics: Solution pushed forward (no TR)

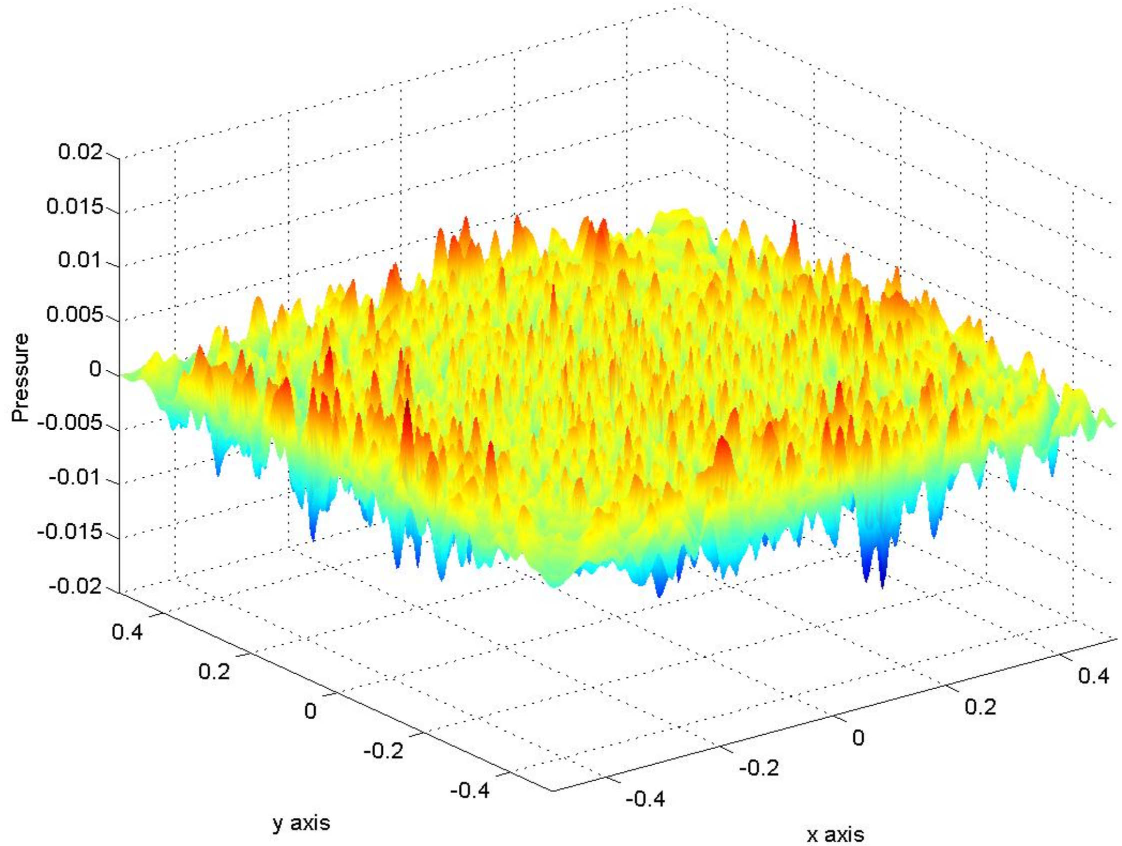

Zoom on Refocused and Original Signals

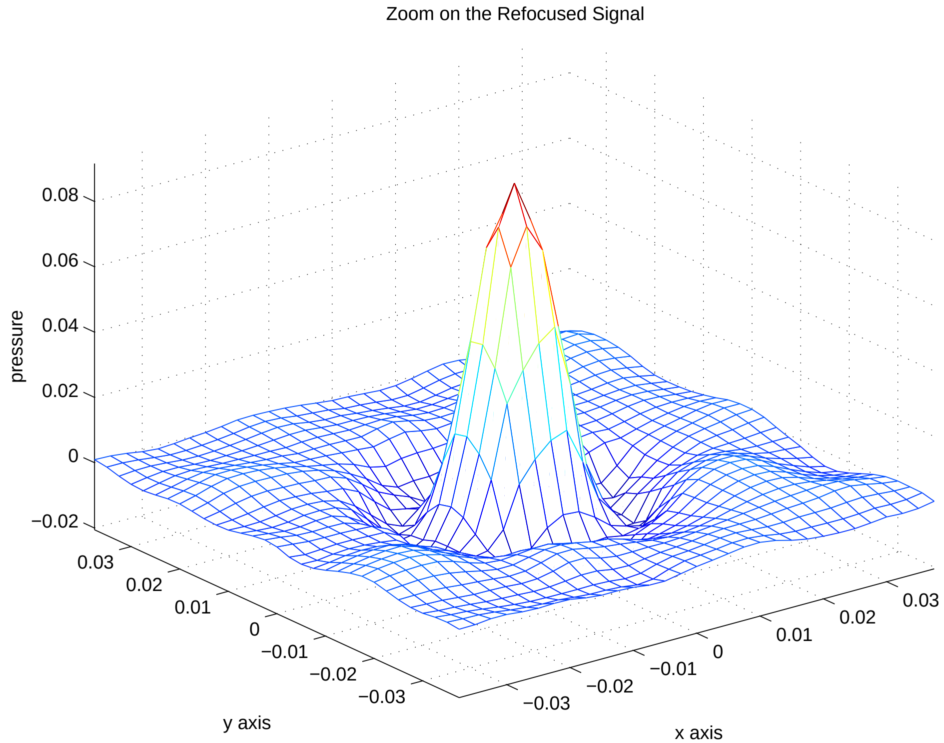

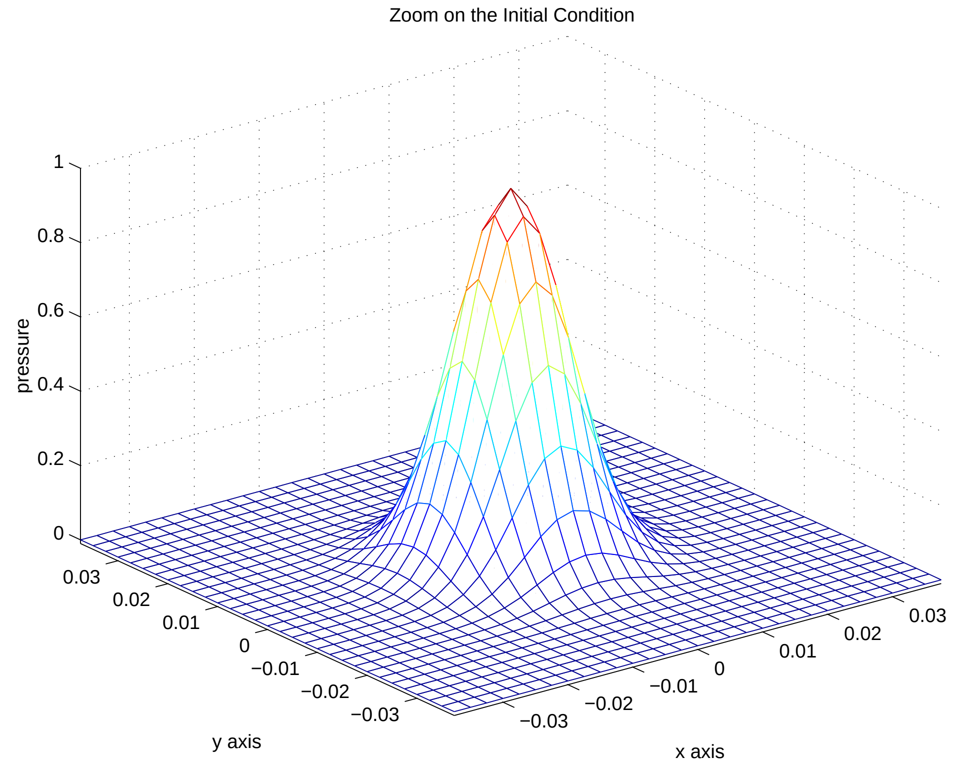

Time-reversal in changing 3D media

We consider time reversal with possibly a change of media between the forward ($\varphi = 1$) and backward ($\varphi = 2$) stages. The forward problem for $\mathbf{u}^\varphi = (\mathbf{v}, p) = (v_1, v_2, v_3, p)$ is

$$A^\varphi(\mathbf{x})\frac{\partial \mathbf{u}^\varphi(t,\mathbf{x})}{\partial t} + D^j \frac{\partial \mathbf{u}^\varphi(t,\mathbf{x})}{\partial x_j} = 0, \quad \mathbf{x} \in \mathbb{R}^3, \qquad \varphi = 1, 2,$$

with initial condition $\mathbf{u}^1(t=0) = \mathbf{u}_0$; $\underline{A^\varphi(\mathbf{x}) = \text{Diag}(\rho, \rho, \rho, \kappa^\varphi(\mathbf{x}))}$.

Using Green's propagators $G^\varphi(t, \mathbf{x}; \mathbf{y})$, the back-propagated signal is

$$\boxed{\mathbf{u}^B(\mathbf{x}) = \int_{\mathbb{R}^9} \Gamma G^2(T, \mathbf{x}; \mathbf{y}) \Gamma G^1(T, \mathbf{y}'; \mathbf{z}) \chi_\Omega(\mathbf{y}) \chi_\Omega(\mathbf{y}') f(\mathbf{y} - \mathbf{y}') \mathbf{u}_0(\mathbf{z}) d\mathbf{y} d\mathbf{y}' d\mathbf{z}.}$$

- $\Gamma = \text{Diag}(-1, -1, -1, 1)$ models the time reversal process
- $\chi_\Omega(\mathbf{y})$ models the array of detectors and $f(\mathbf{y})$ blurring at the detectors
- T is the duration of each propagation stages.

High Frequency scaling

We are interested in high frequency ($O(\varepsilon^{-1})$) wave propagation and thus wish to analyze the refocusing signal at distances $O(\varepsilon)$ away from the source center.

Rescale the problem with $\mathbf{u}_0(\mathbf{x}) = \mathbf{S}\left(\frac{\mathbf{x}-\mathbf{x}_0}{\varepsilon}\right)$ and accordingly with a filter $\frac{1}{\varepsilon^3} f(\frac{\mathbf{y}-\mathbf{y}'}{\varepsilon})$. An observation point $\mathbf{x}$ close to $\mathbf{x}_0$ is written as $\mathbf{x} = \mathbf{x}_0 + \varepsilon \boldsymbol{\xi}$, so that in the new variables

$$\mathbf{u}^B_\varepsilon(\boldsymbol{\xi};\mathbf{x}_0) = \int_{\mathbb{R}^9} \Gamma G^2_\varepsilon(T, \mathbf{x}_0 + \varepsilon\boldsymbol{\xi}; \mathbf{y}) \Gamma G^1_\varepsilon(T, \mathbf{y}'; \mathbf{x}_0 + \varepsilon \mathbf{z}) \times \mathbf{S}(\mathbf{z}) \chi_\Omega(\mathbf{y}) \chi_\Omega(\mathbf{y}') f(\frac{\mathbf{y}-\mathbf{y}'}{\varepsilon}) d\mathbf{y} d\mathbf{y}' d\mathbf{z}.$$

We thus want to understand the limiting properties (as $\varepsilon \to 0$) of the 4×4-matrix $G^2_\varepsilon(T, \mathbf{x}_0 + \varepsilon\boldsymbol{\xi}; \mathbf{y}) \Gamma G^1_\varepsilon(T, \mathbf{y}'; \mathbf{x}_0 + \varepsilon \mathbf{z})$. We use kinetic models for this.

An adjoint Green's matrix

Recall that the Green function $G^1(t,\mathbf{x};\mathbf{y})$ solves the equation

$$A^1\frac{\partial G^1(t,\mathbf{x};\mathbf{y})}{\partial t} + D^j\frac{\partial}{\partial x_j}(G^1(t,\mathbf{x};\mathbf{y})) = 0, \qquad G^1(0,\mathbf{x};\mathbf{y}) = \delta(\mathbf{x}-\mathbf{y})I.$$

Introduce the adjoint Green's matrix G^1_*, solution of

$$\frac{\partial G^1_*(t,\mathbf{x};\mathbf{y})}{\partial t} + \frac{\partial G^1_*(t,\mathbf{x};\mathbf{y})}{\partial x_j}D^j(A^1)^{-1}(\mathbf{x}) = 0,\ G^1_*(0,\mathbf{x};\mathbf{y}) = \delta(\mathbf{x}-\mathbf{y})\Gamma A^{-1}(\mathbf{y})\Gamma.$$

We verify the following Maxwell reciprocity-type result

$$\Gamma G^1(t,\mathbf{y};\mathbf{x}) = G^1_*(t,\mathbf{x};\mathbf{y})A^1(\mathbf{x})\Gamma.$$

This allows us to recast the back-propagated signal as

$$\mathbf{u}^B_\varepsilon(\boldsymbol{\xi};\mathbf{x}_0) = \int_{\mathbb{R}^9} \Gamma G^2_\varepsilon(T,\mathbf{x}_0+\varepsilon\boldsymbol{\xi};\mathbf{y})G^1_{\varepsilon *}(T,\mathbf{x}_0+\varepsilon\mathbf{z};\mathbf{y}')A^1_\varepsilon(\mathbf{x}_0+\varepsilon\mathbf{z})\Gamma \times\mathbf{S}(\mathbf{z})\chi_\Omega(\mathbf{y})\chi_\Omega(\mathbf{y}')f\Big(\frac{\mathbf{y}-\mathbf{y}'}{\varepsilon}\Big)d\mathbf{y}d\mathbf{y}'d\mathbf{z}.$$

Theory of time-reversal refocusing

Introduce now the Wigner transform

$$W_\varepsilon(t,\mathbf{x},\mathbf{k}) = \int_{\mathbb{R}^6} \Big[\int_{\mathbb{R}^3} e^{i\mathbf{k}\cdot\mathbf{z}} G^2_\varepsilon(t,\mathbf{x}-\frac{\varepsilon\mathbf{z}}{2};\mathbf{y}) G^1_{\varepsilon *}(t,\mathbf{x}+\frac{\varepsilon\mathbf{z}}{2};\mathbf{y}')\frac{d\mathbf{z}}{(2\pi)^3}\Big] \times\chi_\Omega(\mathbf{y})\chi_\Omega(\mathbf{y}')f(\frac{\mathbf{y}-\mathbf{y}'}{\varepsilon})d\mathbf{y}d\mathbf{y}',$$

which satisfies the same equation as we have seen before. This allows us to write the refocused signal in terms of the Wigner transform as

$$\boxed{\mathbf{u}^B_\varepsilon(\boldsymbol{\xi};\mathbf{x}_0) = \int_{\mathbb{R}^6} \Gamma W_\varepsilon(t,\mathbf{x}_0+\varepsilon\frac{\boldsymbol{\xi}+\mathbf{z}}{2},\mathbf{k}) e^{-i\mathbf{k}\cdot(\mathbf{z}-\boldsymbol{\xi})} A^1_\varepsilon(\mathbf{x}_0+\varepsilon\mathbf{z})\Gamma\mathbf{S}(\mathbf{z})d\mathbf{z}d\mathbf{k}.}$$

High frequency estimates of refocusing are obtained by analyzing the limit of $W_\varepsilon(t,\mathbf{x},\mathbf{k})$ as $\varepsilon\to 0$: $\boxed{\hat{\mathbf{u}}^B(\mathbf{k};\mathbf{x}_0) = \Gamma W_0(t,\mathbf{x}_0,\mathbf{k})A^1_0(\mathbf{x}_0)\Gamma\hat{\mathbf{S}}(\mathbf{k})}$.

Primer on Wigner Transform

The Wigner transform of two vector fields is defined by:

$$W_\varepsilon[\mathbf{u},\mathbf{v}](\mathbf{x},\mathbf{k}) = \int_{\mathbb{R}^d} e^{i\mathbf{y}\cdot\mathbf{k}}\mathbf{u}(\mathbf{x}-\varepsilon\frac{\mathbf{y}}{2})\mathbf{v}^*(\mathbf{x}+\varepsilon\frac{\mathbf{y}}{2})\frac{d\mathbf{y}}{(2\pi)^d}.$$

It is the inverse Fourier transform of the product:

$$W_\varepsilon[\mathbf{u},\mathbf{v}](\mathbf{x},\mathbf{k}) = \mathcal{F}^{-1}\Big(\mathbf{u}(\mathbf{x}+\varepsilon\frac{\mathbf{y}}{2})\mathbf{v}^*(\mathbf{x}-\varepsilon\frac{\mathbf{y}}{2})\Big).$$

We verify that

$$\begin{aligned}
\int_{\mathbb{R}^d} W[\mathbf{u},\mathbf{v}](\mathbf{x},\mathbf{k})d\mathbf{k} &= (\mathbf{u}\mathbf{v}^*)(\mathbf{x}) \\
\int_{\mathbb{R}^d} \mathbf{k}W[\mathbf{u},\mathbf{v}](\mathbf{x},\mathbf{k})d\mathbf{k} &= \frac{i\varepsilon}{2}(\mathbf{u}\nabla\mathbf{v}^* - \nabla\mathbf{u}\mathbf{v}^*)(\mathbf{x}) \\
\int_{\mathbb{R}^{2d}} |\mathbf{k}|^2 W[\mathbf{u},\mathbf{v}](\mathbf{x},\mathbf{k})d\mathbf{k}d\mathbf{x} &= \varepsilon^2\int_{\mathbb{R}^d}\nabla\mathbf{u}\cdot\nabla\mathbf{v}^* d\mathbf{x}.
\end{aligned}$$

Equations for the Wigner transform

Consider two field equations and the Wigner transform:

$$\varepsilon \frac{\partial \mathbf{u}_\varepsilon^\varphi}{\partial t} + A_\varepsilon^\varphi \mathbf{u}_\varepsilon^\varphi = 0, \qquad \varphi = 1,2, \qquad W_\varepsilon(t,\mathbf{x},\mathbf{k}) = W[\mathbf{u}_\varepsilon^1(t,\cdot),\mathbf{u}_\varepsilon^2(t,\cdot)](\mathbf{x},\mathbf{k}).$$

Then we verify that

$$\varepsilon \frac{\partial W_\varepsilon}{\partial t} + W[A_\varepsilon^1 \mathbf{u}_\varepsilon^1, \mathbf{u}_\varepsilon^2] + W[\mathbf{u}_\varepsilon^1, A_\varepsilon^2 \mathbf{u}_\varepsilon^2] = 0.$$

Calculations of the type

$$W[P(\mathbf{x},\varepsilon\mathbf{D})\mathbf{u},\mathbf{v}](\mathbf{x},\mathbf{k}) = \int_{\mathbb{R}^{3d}} e^{i\mathbf{y}\cdot\boldsymbol{\xi}} e^{i\mathbf{p}\cdot(\mathbf{x}-\mathbf{y})} \hat{\mathbf{P}}(\boldsymbol{\xi}, i\mathbf{k} + i\varepsilon(\frac{\mathbf{p}}{2} - \boldsymbol{\xi})) \underline{W[\mathbf{u},\mathbf{v}]}(\mathbf{y},\mathbf{k} - \frac{\varepsilon\boldsymbol{\xi}}{2})\Big] \frac{d\mathbf{p}\,d\boldsymbol{\xi}\,d\mathbf{y}}{(2\pi)^d}$$

$$W[V(\mathbf{x},\frac{\mathbf{x}}{\varepsilon})\mathbf{u},\mathbf{v}](\mathbf{x},\mathbf{k}) = \int_{\mathbb{R}^{2d}} e^{i\frac{\mathbf{x}\cdot\mathbf{p}}{\varepsilon}} e^{i\mathbf{x}\cdot\mathbf{q}} \widehat{V}(\mathbf{q},\mathbf{p}) \underline{W[\mathbf{u},\mathbf{v}]}(\mathbf{x},\mathbf{k} - \frac{\mathbf{p}}{2} - \frac{\varepsilon\mathbf{q}}{2}) \frac{d\mathbf{p}\,d\mathbf{q}}{(2\pi)^{2d}},$$

allow us to obtain an explicit equation for W_ε. The above formulas are amenable to asymptotic expansions in ε.

Weak-Coupling Regime

In the weak coupling regime, the random fluctuations of the media are modeled by

$$(c_\varepsilon^\varphi)^2(\mathbf{x}) = c_0^2 - \sqrt{\varepsilon} V^\varphi(\frac{\mathbf{x}}{\varepsilon}), \quad \varphi = 1, 2,$$

$$c_0^2 = \frac{1}{\kappa_0 \rho_0}, \qquad V^\varphi(\mathbf{x}) = \frac{c_0^2}{\kappa_0} \kappa_1^\varphi(\mathbf{x}),$$

where c_0 is the average background speed and κ_1^φ and V^φ are random fluctuations in the compressibility and sound speed, respectively. We assume that $V^\varphi(\mathbf{x})$, $\varphi = 1, 2$, are **statistically homogeneous** mean-zero random fields with correlation functions and power spectra given by:

$$\begin{aligned} c_0^4 R^{\varphi\psi}(\mathbf{x}) &= \langle V^\varphi(\mathbf{y}) V^\psi(\mathbf{y}+\mathbf{x}) \rangle, \qquad 1 \leq \varphi, \psi \leq 2, \\ (2\pi)^d c_0^4 \hat{R}^{\varphi\psi}(\mathbf{p}) \delta(\mathbf{p}+\mathbf{q}) &= \langle \hat{V}^\varphi(\mathbf{p}) \hat{V}^\psi(\mathbf{q}) \rangle. \end{aligned}$$

Kinetic theory in weak coupling regime

The Wigner distribution at time $t = 0$ is given by

$$W(0, \mathbf{x}, \mathbf{k}) = |\chi_\Omega(\mathbf{x})|^2 \hat{f}(\mathbf{k}) A_0^{-1}(\mathbf{x}), \text{ where } (A_\varepsilon^\varphi)^{-1} = A_0^{-1} + O(\sqrt{\varepsilon}).$$

The limit Wigner distribution is decomposed as:
$W(t, \mathbf{x}, \mathbf{k}) = a_+(t, \mathbf{x}, \mathbf{k})\mathbf{b}_+\mathbf{b}_+^* + a_-(t, \mathbf{x}, \mathbf{k})\mathbf{b}_-\mathbf{b}_-^*$. Furthermore, the **radiative transfer equation** for a_+ is (with $\omega_+ = c_0|\mathbf{k}|$)

$$\begin{aligned}
& \frac{\partial a_+}{\partial t} + c_0 \hat{\mathbf{k}} \cdot \nabla a_+ + (\Sigma(\mathbf{k}) + i\Pi(\mathbf{k}))a_+ \\
= & \frac{\pi \omega_+^2(\mathbf{k})}{2(2\pi)^d} \int_{\mathbb{R}^d} \hat{R}^{12}(\mathbf{k} - \mathbf{q}) a_+(\mathbf{q}) \delta\Big(\omega_+(\mathbf{q}) - \omega_+(\mathbf{k})\Big) d\mathbf{q}, \\
\Sigma(\mathbf{k}) = & \frac{\pi \omega_+^2(\mathbf{k})}{2(2\pi)^d} \int_{\mathbb{R}^d} \frac{\hat{R}^{11} + \hat{R}^{22}}{2} (\mathbf{k} - \mathbf{q}) \delta\Big(\omega_+(\mathbf{q}) - \omega_+(\mathbf{k})\Big) d\mathbf{q} \\
i\Pi(\mathbf{k}) = & \frac{i\pi \sum_{j=\pm}}{4(2\pi)^d} \text{ p.v.} \int_{\mathbb{R}^d} \Big(\hat{R}^{11} - \hat{R}^{22}\Big)(\mathbf{k} - \mathbf{q}) \frac{\omega_j(\mathbf{k})\omega_+(\mathbf{q})}{\omega_j(\mathbf{q}) - \omega_+(\mathbf{k})} d\mathbf{q}.
\end{aligned}$$

Why is the refocusing stronger in heterogeneous media ?

High frequency approximations of refocusing are given by

$$\boxed{\hat{\mathbf{u}}^B(\mathbf{k};\mathbf{x}_0) = \Gamma W_0(t,\mathbf{x}_0,\mathbf{k}) A_0^1(\mathbf{x}_0)\Gamma\hat{\mathbf{S}}(\mathbf{k})}.$$

where $W(t,\mathbf{x},\mathbf{k}) = a_+(t,\mathbf{x},\mathbf{k})\mathbf{b}_+\mathbf{b}_+^* + a_-(t,\mathbf{x},\mathbf{k})\mathbf{b}_-\mathbf{b}_-^*$.

Thus, the smoother the filter, the less distorted the back-propagated signal $\mathbf{u}^B$. $W_0(t,\mathbf{x}_0,\mathbf{k})$, which solves the radiative transfer equation, is all the smoother that scattering (proportional to $\hat{R}_{12}$) is strong.

In homogeneous media, $W_0(t,\mathbf{x}_0,\mathbf{k})$ is very singular and the backpropagated signal very distorted, leading to poor refocusing. When the two media are strongly correlated (so that $\hat{R}_{12}$ is large), $W_0(t,\mathbf{x}_0,\mathbf{k})$ is smooth and refocusing is enhanced.

Outline

1. Time Reversal in random media and kinetic models

2. **<u>Statistical stability and rigorous theories</u>**

3. Validity of Radiative Transfer Models

4. Applications to Detection and Imaging

Statistical stability in Time Reversal

There are few theoretical results in the weak coupling regime for the wave equation and they are concerned with ensemble averages of the Wigner transform, not its limiting law.

However such limiting laws are accessible for simplifed regimes of radiative transfer, including paraxial approximations, Itô-Schrödinger approximations, and random Liouville equations.

Such limiting laws directly translate into results on the statistical stability of the time reversed signals whether the underlying media change or not between the two stages of the time reversal experiment.

Two models where stability can be proved

• Paraxial (a.k.a. Parabolic) Approximation. Here, we obtain a (quantum) wave equation with *mixing* time dependent coefficients. For a typical wavelength (width of initial pulse) of order $\varepsilon \ll 1$, the fluctuations are of the form

$$\sqrt{\varepsilon} V(\frac{\mathbf{x}}{\varepsilon}, \frac{z}{\varepsilon}).$$

• Random Liouville Equations. Here the high frequency limit of the wave equation (Liouville equation) with *random Hamiltonian* is used to show that the Wigner transform solves in the limit $\varepsilon \to 0$ a Fokker-Planck equation. For a typical wavelength of order $\varepsilon \ll 1$, the fluctuations are of the form

$$\sqrt{\delta(\varepsilon)} V(\frac{\mathbf{x}}{\delta(\varepsilon)}), \quad C |\ln \varepsilon|^{-2/3+\eta} \ll \delta(\varepsilon) \to 0 \qquad \text{as } \varepsilon \to 0.$$

PART 2.1: PARAXIAL APPROXIMATION

Analysis for the Paraxial Equation

The pressure field $p(z, \mathbf{x}, t)$ satisfies the scalar wave equation

$$\frac{1}{c^2(z, \mathbf{x})} \frac{\partial^2 p}{\partial t^2} - \Delta p = 0. \tag{1}$$

The parabolic approximation consists of

$$p(z, \mathbf{x}, t) \approx \int_{\mathbb{R}} e^{i(-c_0 \kappa t + \kappa z)} \psi(z, \mathbf{x}, \kappa) c_0 d\kappa,$$

where ψ satisfies the Schrödinger equation

$$2i\kappa \frac{\partial \psi}{\partial z}(z, \mathbf{x}, \kappa) + \Delta_{\mathbf{x}} \psi(z, \mathbf{x}, \kappa) + \kappa^2 (n^2(z, \mathbf{x}) - 1) \psi(z, \mathbf{x}, \kappa) = 0,$$
$$\psi(z = 0, \mathbf{x}, \kappa) = \psi_0(\mathbf{x}, \kappa)$$

with $\Delta_{\mathbf{x}}$ the transverse Laplacian in the variable $\mathbf{x}$. The refraction index $n(z, \mathbf{x}) = c_0 / c(z, \mathbf{x})$, and c_0 is a reference speed.

Cartoon of Paraxial Approximation

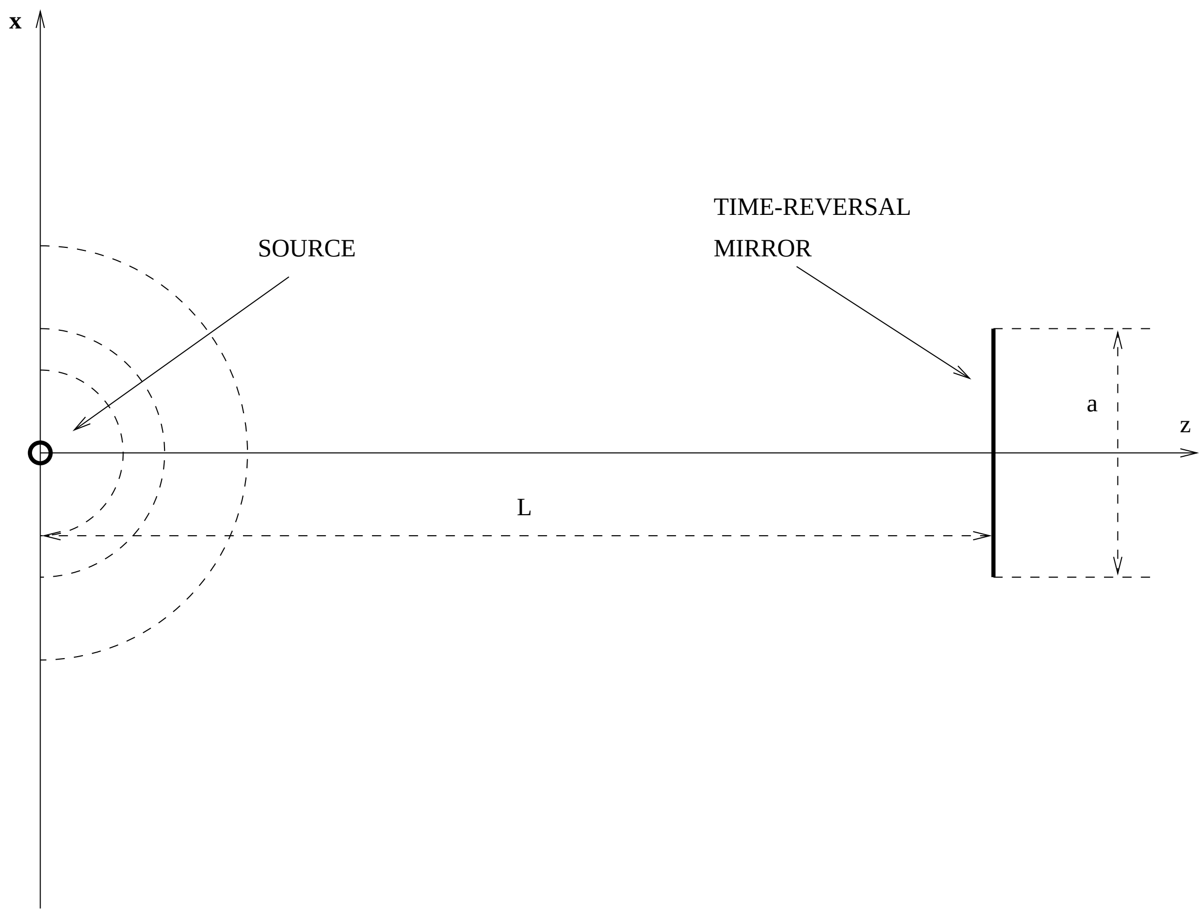

Time Reversal within Paraxial Approximation

The back-propagated signal can be written as

$$\psi^B(\mathbf{x},\kappa) = \int_{\mathbb{R}^{3d}} G^*(L,\mathbf{x},\kappa;\boldsymbol{\eta})G(L,\mathbf{y},\kappa;\mathbf{y}')\chi(\boldsymbol{\eta})\chi(\mathbf{y})f(\boldsymbol{\eta}-\mathbf{y})\psi_0(\mathbf{y}',\kappa)d\mathbf{y}d\mathbf{y}'d\boldsymbol{\eta}.$$

After introduction of the Wigner Transform and scaling, we get

$$\psi_\varepsilon^B(\boldsymbol{\xi},\kappa;\mathbf{x}_0) = \int_{\mathbb{R}^{2d}} e^{i\mathbf{k}\cdot(\boldsymbol{\xi}-\mathbf{y})}W_\varepsilon(L,\mathbf{x}_0+\varepsilon\frac{\mathbf{y}+\boldsymbol{\xi}}{2},\mathbf{k},\kappa)\psi_0(\mathbf{y},\kappa)\frac{d\mathbf{y}d\mathbf{k}}{(2\pi)^d}.$$

The above formula shows that the asymptotic behavior of $\psi_\varepsilon^B(\boldsymbol{\xi},\kappa;\mathbf{x}_0)$ as $\varepsilon\to 0$ is characterized by that of the Wigner transform $W_\varepsilon(L,\mathbf{x},\mathbf{k},\kappa)$.

Scaling and random medium

The scaled Schrödinger equation is

$$2i\kappa\varepsilon\frac{\partial\psi_\varepsilon}{\partial z} + \varepsilon^2\Delta_{\mathbf{x}}\psi_\varepsilon + \kappa^2\sqrt{\varepsilon}V(\frac{\mathbf{x}}{\varepsilon}, \frac{z}{\varepsilon})\psi_\varepsilon = 0,$$
$$\psi_\varepsilon(z=0,\mathbf{x},\kappa) = \psi_0(\mathbf{x},\kappa).$$

The random field $V(z,\mathbf{x})$ is a Markov process in z with infinitesimal generator Q. It is stationary in z and $\mathbf{x}$ with correlation function $R(z,\mathbf{x})$

$$\mathbb{E}\{V(s,\mathbf{y})V(z+s,\mathbf{x}+\mathbf{y})\} = R(z,\mathbf{x}) \quad \text{for all } \mathbf{x},\mathbf{y}\in\mathbb{R}^d, \text{ and } z,s\in\mathbb{R}.$$

The generator Q is a bounded operator on $L^\infty(\mathcal{V})$ with a unique invariant measure $\pi(\hat{V})$, i.e. $Q^*\pi = 0$, and there exists $\alpha > 0$ such that if $\langle g,\pi\rangle = 0$ then

$$\|e^{rQ}g\|_{L^\infty_{\mathcal{V}}} \leq C\|g\|_{L^\infty_{\mathcal{V}}}e^{-\alpha r}.$$

Equation for the Wigner Transform

$$\frac{\partial W_\varepsilon}{\partial z} + \frac{1}{\kappa}\mathbf{k}\cdot\nabla_{\mathbf{x}} W_\varepsilon = \kappa \mathcal{L}_\varepsilon W_\varepsilon$$
$$W_\varepsilon(0,\mathbf{x},\mathbf{k};\kappa) = W_\varepsilon^0(\mathbf{x},\mathbf{k};\kappa),$$

$$\mathcal{L}_\varepsilon W_\varepsilon = \frac{1}{i\sqrt{\varepsilon}}\int_{\mathbb{R}^d} \frac{d\tilde{V}(\frac{z}{\varepsilon},\mathbf{p})}{(2\pi)^d} e^{i\mathbf{p}\cdot\mathbf{x}/\varepsilon}\left[W_\varepsilon(\mathbf{x},\mathbf{k}-\frac{\mathbf{p}}{2}) - W_\varepsilon(\mathbf{x},\mathbf{k}+\frac{\mathbf{p}}{2})\right].$$

The initial condition is given by

$$W_\varepsilon^0(\mathbf{x},\mathbf{k};\kappa) = \int_{\mathbb{R}^d} \frac{e^{i(\mathbf{k}+\mathbf{q})\cdot\mathbf{y}}}{(2\pi)^d}\chi(\mathbf{x}-\frac{\varepsilon\mathbf{y}}{2})\chi(\mathbf{x}+\frac{\varepsilon\mathbf{y}}{2})\hat{f}(\mathbf{q})d\mathbf{y}d\mathbf{q}.$$

It is uniformly bounded in $L^2(\mathbb{R}^d\times\mathbb{R}^d)$ (hence so is $W_\varepsilon(z;\kappa)$) and converges as $\varepsilon\to 0$ to $W^0(\mathbf{x},\mathbf{k};\kappa) = |\chi(\mathbf{x})|^2\hat{f}(\mathbf{k})$.

Main stability result

Let the array $\chi(\mathbf{y})$ and the *filter* $f(\mathbf{y})$ *be in* $L^1 \cap L^\infty(\mathbb{R}^d)$, while $\psi_0 \in L^2(\mathbb{R}^d)$ for a given $\kappa \in \mathbb{R}$. The refraction index $n(z,\mathbf{x})$ satisfies assumptions given above. Then for each $\boldsymbol{\xi} \in \mathbb{R}^d$ the back-propagated signal $\psi_\varepsilon^B(\boldsymbol{\xi}, \mathbf{x}_0, \kappa)$ converges in probability and weakly in $L^2_{\mathbf{x}_0}(\mathbb{R}^d)$ as $\varepsilon \to 0$ to the deterministic

$$\psi^B(\boldsymbol{\xi}, \kappa; \mathbf{x}_0) = \int_{\mathbb{R}^{2d}} e^{i\mathbf{k}\cdot(\boldsymbol{\xi}-\mathbf{y})} \overline{W}(L, \mathbf{x}_0, \mathbf{k}, \kappa) \psi_0(\mathbf{y}, \kappa) \frac{d\mathbf{y}\, d\mathbf{k}}{(2\pi)^d}.$$

The function $\overline{W}$ satisfies the transport equation

$$\frac{\partial \overline{W}}{\partial z} + \frac{1}{\kappa}\mathbf{k} \cdot \nabla_{\mathbf{x}} \overline{W} = \kappa \mathcal{L} \overline{W},$$

with initial data $\overline{W}_0(\mathbf{x}, \mathbf{k}) = \hat{f}(\mathbf{k}) |\chi(\mathbf{x})|^2$ and operator $\mathcal{L}$ defined by

$$\mathcal{L}\lambda = \int_{\mathbb{R}^d} \frac{d\mathbf{p}}{(2\pi)^d} \hat{R}\Big(\frac{|\mathbf{p}|^2 - |\mathbf{k}|^2}{2}, \mathbf{p} - \mathbf{k}\Big)(\lambda(\mathbf{p}) - \lambda(\mathbf{k})),$$

where $\hat{R}(\omega, \mathbf{p})$ is the Fourier transform of the correlation function of V.

Result on the Wigner transform

Under the same assumptions, the Wigner distribution W_ε converges *in probability and weakly* in $L^2(\mathbb{R}^{2d})$ to the solution $\overline{W}$ of the above transport equation. More precisely, for any test function $\lambda \in L^2(\mathbb{R}^{2d})$ the process $\langle W_\varepsilon(z), \lambda \rangle$ converges to $\langle \overline{W}(z), \lambda \rangle$ in probability as $\varepsilon \to 0$, uniformly on finite intervals $0 \leq z \leq L$.

Here, $\langle \cdot, \cdot \rangle$ is the usual scalar product in $L^2(\mathbb{R}^{2d})$.

Details of the proofs

The scaling of the random fluctuations is supposed to be $\sqrt{\varepsilon}V(\frac{\mathbf{x}}{\varepsilon},\frac{z}{\varepsilon})$.

We then have the following equation for the scaled W_ε:

$$\frac{\partial W_\varepsilon}{\partial z} + \mathbf{k}\cdot\nabla_{\mathbf{x}} W_\varepsilon = \mathcal{L}_\varepsilon W_\varepsilon$$
$$W_\varepsilon(0,\mathbf{x},\mathbf{k}) = W_\varepsilon^0(\mathbf{x},\mathbf{k}),$$

with

$$\mathcal{L}_\varepsilon W_\varepsilon = \frac{1}{i\sqrt{\varepsilon}}\int_{\mathbb{R}^d} \frac{d\tilde{V}(\frac{z}{\varepsilon},\mathbf{p})}{(2\pi)^d} e^{i\mathbf{p}\cdot\mathbf{x}/\varepsilon}\Big[W_\varepsilon(\mathbf{x},\mathbf{k}-\frac{\mathbf{p}}{2}) - W_\varepsilon(\mathbf{x},\mathbf{k}+\frac{\mathbf{p}}{2})\Big].$$

Thanks to the blurring at the detectors, we obtain uniform bounds in L^2 for the Wigner transform W_ε independently of the realization of the random medium.

Construction of approximate martingales

Let us define P_ε as the probability measure on the space of paths $C([0,L];X)$ generated by V_ε and W_ε. Let $\lambda(z,\mathbf{x},\mathbf{k})$ be a deterministic test function. We use the Markovian property of the random field $V(z,\mathbf{x})$ in z to construct a first functional $G_\lambda : C([0,L];X) \to C[0,L]$ by

$$G_\lambda[W](z) = \langle W,\lambda\rangle(z) - \int_0^z \langle W, \frac{\partial\lambda}{\partial z} + \mathbf{k}\cdot\nabla_{\mathbf{x}}\lambda + \mathcal{L}\lambda\rangle(\zeta)d\zeta$$

and show that it is an approximate P_ε-martingale, more precisely

$$\left|\mathbb{E}^{P_\varepsilon}\left\{G_\lambda[W](z)|\mathcal{F}_s\right\} - G_\lambda[W](s)\right| \le C_{\lambda,L}\sqrt{\varepsilon}$$

uniformly for all $W \in C([0,L];X)$ and $0 \le s < z \le L$. Then there exists a subsequence $\varepsilon_j \to 0$ so that P_{ε_j} converges weakly to a measure P supported on $C([0,L];X)$. Weak convergence of P_ε and the above error estimate together imply that $G_\lambda[W](z)$ is a P-martingale so that

$$\mathbb{E}^P\left\{G_\lambda[W](z)|\mathcal{F}_s\right\} - G_\lambda[W](s) = 0.$$

Taking $s = 0$ above we obtain the transport equation for $\overline{W} = \mathbb{E}^P \{W(z)\}$ in its weak formulation.

The second step is to show that for every test function $\lambda(z, \mathbf{x}, \mathbf{k})$ the new functional

$$G_{2,\lambda}[W](z) = \langle W, \lambda \rangle^2(z) - 2\int_0^z \langle W, \lambda \rangle(\zeta) \langle W, \frac{\partial \lambda}{\partial z} + \mathbf{k} \cdot \nabla_{\mathbf{x}} \lambda + \mathcal{L}\lambda \rangle(\zeta) d\zeta$$

is also an approximate P_ε-martingale. We then obtain that $\mathbb{E}^{P_\varepsilon} \left\{ \langle W, \lambda \rangle^2 \right\} \to \langle \overline{W}, \lambda \rangle^2$, which implies convergence in probability. It follows that the limit measure P is unique and deterministic, and that the whole sequence P_ε converges.

That $G_{2,\lambda}[W](z)$ is an approximate P_ε-martingale uses very explicitly the uniform a priori L^2 bound on the Wigner distribution W_ε.

PART 2.2: ITO SCHRÖDINGER APPROXIMATION

Itô Schrödinger equations

Let us come back to the parabolic approximation

$$\frac{\partial\psi}{\partial z} + \frac{-iL_z}{2kL_x^2}\Delta_{\mathbf{x}}\psi = \frac{ikL_z\nu}{2}\mu(\frac{L_x\mathbf{x}}{l_x}, \frac{L_z z}{l_z})\psi.$$

We now assume that the variations in z are very fast: $l_z \ll \lambda$. Then we can formally replace

$$\frac{kL_z\nu}{2}\mu(\frac{L_x\mathbf{x}}{l_x}, \frac{L_z z}{l_z})dz \qquad \text{by} \qquad \kappa B(\frac{L_x\mathbf{x}}{l_x}, dz),$$

where $B(\mathbf{x}, dz)$ is the usual Wiener measure in z with statistics

$$\langle B(\mathbf{x}, z)B(\mathbf{y}, z')\rangle = Q(\mathbf{y}-\mathbf{x})z \wedge z'.$$

Itô Schrödinger equation

The parabolic equation in this regime becomes then

$$d\psi(\mathbf{x},z) = \frac{iL_z}{2kL_x^2}\Delta_{\mathbf{x}}\psi(\mathbf{x},z)dz + i\kappa\psi(\mathbf{x},z)\circ B(\frac{L_x\mathbf{x}}{l_x},dz).$$

Here $\circ$ means that the stochastic equation is understood in the Stratonovich sense. In the Itô sense it becomes the Itô-Schrödinger equation:

$$d\psi(\mathbf{x},z) = \frac{1}{2}\Big(\frac{iL_z}{kL_x^2}\Delta_{\mathbf{x}} - \kappa^2 Q(\mathbf{0})\Big)\psi(\mathbf{x},z)dz + i\kappa\psi(\mathbf{x},z)B(\frac{L_x\mathbf{x}}{l_x},dz).$$

Advantage: Closed equations for the statistical moments.

First moment

The first moment defined by $m_1(\mathbf{x}, z) = \langle \psi(\mathbf{x}, z) \rangle$ satisfies

$$\frac{\partial m_1}{\partial z}(\mathbf{x}, z) = \frac{1}{2}\Big(\frac{iL_z}{kL_x^2}\Delta_{\mathbf{x}} - Q(\mathbf{0})\Big)m_1(\mathbf{x}, z).$$

The L^2 norm of the first moment

$$M_2(z) = \Big(\int_{\mathbb{R}^d} |m_1(\mathbf{x}, z)|^2 d\mathbf{x}\Big)^{1/2}.$$

is given by

$$M_2(z) = e^{-\frac{Q(\mathbf{0})}{2}z} M_2(0).$$

This shows that the coherent field m_1 decays exponentially in z. This exponential decay is *not* related to intrinsic absorption. Instead it describes the loss of coherence caused by multiple scattering.

Second Moment (I)

Energy propagation is better understood by looking at the second moment

$$\tilde{m}_2(\mathbf{x}_1, \mathbf{x}_2, z) = \langle \psi(\mathbf{x}_1, z)\psi^*(\mathbf{x}_2, z)\rangle.$$

By application of the Itô formula we have

$$\begin{aligned} d(\psi(\mathbf{x}_1, z)\psi^*(\mathbf{x}_2, z)) = \psi(\mathbf{x}_1, z) d\psi^*(\mathbf{x}_2, z) \\ + d\psi(\mathbf{x}_1, z)\psi^*(\mathbf{x}_2, z) + d\psi(\mathbf{x}_1, z) d\psi^*(\mathbf{x}_2, z). \end{aligned}$$

This implies that

$$\frac{\partial \tilde{m}_2}{\partial z} = \frac{iL_z}{2kL_x^2}(\Delta_{\mathbf{x}_1} - \Delta_{\mathbf{x}_2})\tilde{m}_2 + \Big(Q\Big(\frac{L_x(\mathbf{x}_1 - \mathbf{x}_2)}{l_x}\Big) - Q(\mathbf{0})\Big)\tilde{m}_2.$$

Second Moment (II)

Introduce the rescaled variables: $\mathbf{x} = \dfrac{\mathbf{x}_1 + \mathbf{x}_2}{2}$, $\quad \mathbf{y} = \dfrac{\mathbf{x}_1 - \mathbf{x}_2}{\eta}$. Here the adimensionalized wavelength $\varepsilon \ll \eta \ll 1$. Defining $m_2(\mathbf{x}, \mathbf{y}) = \tilde{m}_2(\mathbf{x}_1, \mathbf{x}_2)$ we have

$$\frac{\partial m_2}{\partial z} = \frac{iL_z}{kL_x^2\eta} \nabla_{\mathbf{x}} \cdot \nabla_{\mathbf{y}} m_2(z) - \Big(Q(\mathbf{0}) - Q(\mathbf{y})\Big) m_2(z).$$

Introduce the Wigner transform

$$W(\mathbf{x}, \mathbf{p}, z) = \frac{1}{(2\pi)^d} \int_{\mathbb{R}^d} e^{i\mathbf{p}\cdot\mathbf{y}} \psi(\mathbf{x} - \frac{\eta \mathbf{y}}{2}, z) \psi^*(\mathbf{x} + \frac{\eta \mathbf{y}}{2}, z) d\mathbf{y}.$$

Then $m_2(\mathbf{x}, \mathbf{y}, z) = \int_{\mathbb{R}^d} e^{i\mathbf{p}\cdot\mathbf{y}} \langle W \rangle (\mathbf{x}, \mathbf{p}, z) d\mathbf{p}$ and

$$\frac{\partial \langle W \rangle}{\partial z} + \frac{L_z}{kL_x^2\eta} \mathbf{p} \cdot \nabla_{\mathbf{x}} \langle W \rangle = \int_{\mathbb{R}^d} \Big[\hat{Q}(\mathbf{p} - \mathbf{p}') - Q(\mathbf{0}) \delta(\mathbf{p} - \mathbf{p}')\Big] \langle W \rangle (\mathbf{p}') d\mathbf{p}'.$$

We thus get an equation for the limiting Wigner transform for free.

Scintillation (moment of order 4)

We can similarly obtain an equation for the fourth moment:

$$\tilde{m}_4(\mathbf{x}_1, \mathbf{x}_2, \mathbf{x}_3, \mathbf{x}_4, z) = \langle \psi(\mathbf{x}_1, z)\psi^*(\mathbf{x}_2, z)\psi(\mathbf{x}_3, z)\psi^*(\mathbf{x}_4, z)\rangle.$$

We introduce the change of variables $m_4(\mathbf{x}, \mathbf{y}, \mathbf{z}, \mathbf{t}, z) = \tilde{m}_4(\mathbf{x}_1, \mathbf{x}_2, \mathbf{x}_3, \mathbf{x}_4, z)$, where $\mathbf{x} = \frac{\mathbf{x}_1 + \mathbf{x}_2}{2}$, $\mathbf{y} = \frac{\mathbf{x}_1 - \mathbf{x}_2}{\eta}$, $\boldsymbol{\xi} = \frac{\mathbf{x}_3 + \mathbf{x}_4}{2}$, $\mathbf{t} = \frac{\mathbf{x}_3 - \mathbf{x}_4}{\eta}$, $\eta = \frac{l_x}{L_x}$. We obtain

$$\frac{\partial m_4}{\partial z} = \frac{iL_z}{kL_x^2 \eta}(\nabla_{\mathbf{x}} \cdot \nabla_{\mathbf{y}} + \nabla_{\boldsymbol{\xi}} \cdot \nabla_{\mathbf{t}}) m_4(z) - \mathcal{Q} m_4(z),$$

$$\mathcal{Q}(\mathbf{x}, \mathbf{y}, \boldsymbol{\xi}, \mathbf{t}) = \Big(2Q(\mathbf{0}) - Q(\mathbf{y}) - Q(\mathbf{t}) + \sum_{\epsilon_i, \epsilon_j = \pm} \epsilon_i \epsilon_j Q(\frac{\mathbf{x} - \boldsymbol{\xi}}{\eta} + \epsilon_i \mathbf{y} - \epsilon_j \mathbf{t})\Big).$$

Scintillation = second moment for the WT

Define $\mathcal{W}(\mathbf{x},\mathbf{p},\boldsymbol{\xi},\mathbf{q},z) = W(\mathbf{x},\mathbf{p},z)W(\boldsymbol{\xi},\mathbf{q},z)$.
Its statistical average can be related to m_4 and we find that

$$\boxed{\frac{\partial\langle\mathcal{W}\rangle}{\partial z} + \frac{L_z}{kL_x^2\eta}(\mathbf{p}\cdot\nabla_{\mathbf{x}} + \mathbf{q}\cdot\nabla_{\boldsymbol{\xi}})\langle\mathcal{W}\rangle = \mathcal{R}_2\langle\mathcal{W}\rangle + K_{12}\langle\mathcal{W}\rangle}$$

$$\begin{aligned}
K_{12}\mathcal{W} &= \int_{\mathbb{R}^d}\hat{Q}(\mathbf{u})e^{i\frac{(\mathbf{x}-\boldsymbol{\xi})\cdot\mathbf{u}}{\eta}}\Big(\mathcal{W}(\mathbf{p}-\tfrac{\mathbf{u}}{2},\mathbf{q}-\tfrac{\mathbf{u}}{2}) + \mathcal{W}(\mathbf{p}+\tfrac{\mathbf{u}}{2},\mathbf{q}+\tfrac{\mathbf{u}}{2}) \\
&\qquad -\mathcal{W}(\mathbf{p}-\tfrac{\mathbf{u}}{2},\mathbf{q}+\tfrac{\mathbf{u}}{2}) - \mathcal{W}(\mathbf{p}+\tfrac{\mathbf{u}}{2},\mathbf{q}-\tfrac{\mathbf{u}}{2})\Big)d\mathbf{u} \\
K_2\mathcal{W} &= \int_{\mathbb{R}^{2d}}\Big[\hat{Q}(\mathbf{p}-\mathbf{p}')\delta(\mathbf{q}-\mathbf{q}') + \hat{Q}(\mathbf{q}-\mathbf{q}')\delta(\mathbf{p}-\mathbf{p}')\Big]\mathcal{W}(\mathbf{p}',\mathbf{q}')d\mathbf{p}'d\mathbf{q}' \\
\mathcal{R}_2\mathcal{W} &= K_2\mathcal{W} - 2Q(\mathbf{0})\mathcal{W}.
\end{aligned}$$

When the phase term cancels so that "$|K_{12}\mathcal{W}| \ll 1$", we obtain that

$$\boxed{J_\eta(\mathbf{x},\mathbf{p},\boldsymbol{\xi},\mathbf{q},z) = \langle\mathcal{W}(\mathbf{x},\mathbf{p},\boldsymbol{\xi},\mathbf{q},z)\rangle - \langle W(\mathbf{x},\mathbf{p},z)\rangle\,\langle W(\boldsymbol{\xi},\mathbf{q},z)\rangle},$$

the scintillation function, is small. The energy is then statistically stable.

Smallness of the scintillation function

Theorem. Let us assume that $W_\eta(\mathbf{x},\mathbf{p},0)$ is deterministic and such that

$$\int_{\mathbb{R}^{2d}} |W_\eta(\mathbf{x},\mathbf{p},0)|^2 d\mathbf{x}d\mathbf{p} + \int_{\mathbb{R}^d} \sup_{\mathbf{x}} |W_\eta(\mathbf{x},\mathbf{p},0)|^2 d\mathbf{p} \leq C,$$

where C is a constant independent of η. Assume also that the correlation function $Q(\mathbf{x}) \in L^1(\mathbb{R}^d) \cap L^\infty(\mathbb{R}^d)$. Then

$$\|J_\eta\|_2(z) \leq C\eta^{d/2},$$

uniformly in z on compact intervals.

Weak statistical stability

Theorem. Under the assumptions of the previous theorem and $\lambda \in L^2(\mathbb{R}^{2d})$, we obtain that

$$\left\langle \left\{ \Big((W_\eta, \lambda) - (\langle W_\eta \rangle, \lambda) \Big)^2 \right\} \right\rangle \leq C\eta^{d/2} \|\lambda\|_2^2.$$

Also (W_η, λ) becomes deterministic in the limit of small values of η as

$$P\Big(\Big| (W_\eta, \lambda) - (\langle W_\eta \rangle, \lambda) \Big| \geq \alpha \Big) \leq \frac{C\eta^{d/2}\|\lambda\|_2^2}{\alpha^2} \to 0 \qquad \text{as } \eta \to 0.$$

The Wigner transform W_η of the stochastic field ψ_η converges weakly and in probability to the deterministic solution $\overline{W}(\mathbf{x}, \mathbf{p}, z)$ of a Radiative Transfer Equation.

Application to Time Reversal

Theorem. Assume that the initial condition $\psi_0(\mathbf{y}) \in L^2(\mathbb{R}^d)$, the filter $f(\mathbf{y}) \in L^1(\mathbb{R}^d) \cap L^2(\mathbb{R}^d)$, and the detector amplification $\chi(\mathbf{x})$ is sufficiently smooth. Then $\psi_\eta^B(\boldsymbol{\xi}; \mathbf{x}_0)$ converges weakly and in probability to the deterministic *back-propagated signal*

$$\psi^B(\boldsymbol{\xi}; \mathbf{x}_0) = \int_{\mathbb{R}^d} e^{i\mathbf{k}\cdot\boldsymbol{\xi}} \overline{W}(\mathbf{x}_0, \mathbf{k}, L) \hat{\psi}_0(\mathbf{k}) d\mathbf{k},$$

where $\overline{W}(\mathbf{x}_0, \mathbf{k}, L)$ is the solution of a RTE with initial conditions $\overline{W}(\mathbf{x}, \mathbf{k}, 0) = \hat{f}(\mathbf{k})|\chi(\mathbf{x})|^2$. Moreover introducing $\lambda(\boldsymbol{\xi}, \mathbf{x}_0) = \tilde{\lambda}(\mathbf{x}_0)\mu(\boldsymbol{\xi})$ we have the following estimate

$$\left\langle (\psi_\eta^B - \langle \psi_\eta^B \rangle, \lambda)^2 \right\rangle \le C\eta^d \|\psi_0\|_2^2 \|\lambda\|_2^2 = C\eta^d \|\psi_0\|_2^2 \|\mu\|_2^2 \|\tilde{\lambda}\|_2^2,$$

uniformly in L on compact intervals.

We *do not* have such an estimate for the *parabolic* approximation.

Scintillation may appear and not disappear

Theorem. Assume that $W_\eta(\mathbf{x},\mathbf{p},0)=\delta(\mathbf{x}-\mathbf{x}_0)\delta(\mathbf{p}-\mathbf{p}_0)$ [not physical in Time Reversal]. Then the scintillation function J_η is composed of a singular term of the form (with $Q=Q(\mathbf{0})$):

$$\delta(\mathbf{x}-\boldsymbol{\xi})\delta(\mathbf{p}-\mathbf{q})\Big(\alpha(\mathbf{x},\mathbf{p},z)-e^{-2Qz}\alpha(\mathbf{x}-z\mathbf{p},\mathbf{p},0)\Big)$$

plus other contributions that are mutually singular with respect to this term. Moreover the density $\alpha(\mathbf{x},\mathbf{p},z)$ solves the radiative transfer equation with initial condition $a_0(\mathbf{x},\mathbf{p})=\delta(\mathbf{x}-\mathbf{x}_0)\delta(\mathbf{p}-\mathbf{p}_0)$:

$$\frac{\partial\alpha}{\partial z}+\mathbf{p}\cdot\nabla_{\mathbf{x}}\alpha+2Q\alpha=\int_{\mathbb{R}^d}\hat{Q}(\mathbf{u})\Big(\alpha(\mathbf{x},\mathbf{p}+\frac{\mathbf{u}}{2},z)+\alpha(\mathbf{x},\mathbf{p}-\frac{\mathbf{u}}{2},z)\Big)d\mathbf{u}.$$

The total intensity of this scintillation is $(1-e^{-2Qz})$ (so it grows in z though it vanishes at $z=0$).

In this case *Energy* is NOT statistically stable.

PART 2.3: RANDOM LIOUVILLE REGIME

Stability by Random Liouville

Let us come back to the full wave equation and introduce $\mathbf{v}_\varepsilon(t,\mathbf{x}) = A_\varepsilon^{1/2}(\mathbf{x})\mathbf{u}_\varepsilon(t,\mathbf{x})$ that satisfies the symmetrized system

$$\frac{\partial \mathbf{v}_\varepsilon}{\partial t} + A_\varepsilon^{-1/2}(\mathbf{x}) D^j \frac{\partial}{\partial x^j}\Big(A_\varepsilon^{-1/2}(\mathbf{x})\mathbf{v}_\varepsilon(\mathbf{x})\Big) = 0.$$

Define $P_\varepsilon(\mathbf{x},\mathbf{k}) = P_0(\mathbf{x},\mathbf{k}) + \varepsilon P_1(\mathbf{x})$, where

$$P_0(\mathbf{x},\mathbf{k}) = iA_\varepsilon^{-\frac{1}{2}}(\mathbf{x}) D^j A_\varepsilon^{-\frac{1}{2}}(\mathbf{x}) k_j = ic_\varepsilon(\mathbf{x}) k_j D^j$$
$$2P_1(\mathbf{x}) = A_\varepsilon^{-\frac{1}{2}}(\mathbf{x}) D^j \frac{\partial}{\partial x_j}\Big(A_\varepsilon^{-\frac{1}{2}}(\mathbf{x})\Big) - \frac{\partial}{\partial x_j}\Big(A_\varepsilon^{-\frac{1}{2}}(\mathbf{x})\Big) D^j A_\varepsilon^{-\frac{1}{2}}(\mathbf{x}).$$

The Wigner transform $W_\varepsilon(t,\mathbf{x},\mathbf{k})$ satisfies the evolution equation

$$\varepsilon \frac{\partial W_\varepsilon}{\partial t} + \mathcal{L}_\varepsilon W_\varepsilon = 0$$
$$\mathcal{L}_\varepsilon f(\mathbf{x},\mathbf{k}) = \int \Big(P_\varepsilon(\mathbf{y},\mathbf{q}) e^{i\phi} f(\mathbf{z},\mathbf{p}) - f(\mathbf{z},\mathbf{p}) e^{-i\phi} P_\varepsilon(\mathbf{y},\mathbf{q})\Big) \frac{d\mathbf{z}d\mathbf{p}d\mathbf{y}d\mathbf{q}}{(\pi\varepsilon)^{2d}},$$
$$\phi(\mathbf{x},\mathbf{z},\mathbf{k},\mathbf{p},\mathbf{y},\mathbf{q}) = \tfrac{2}{\varepsilon}((\mathbf{p}-\mathbf{k})\cdot\mathbf{y} + (\mathbf{q}-\mathbf{p})\cdot\mathbf{x} + (\mathbf{k}-\mathbf{q})\cdot\mathbf{z}).$$

The Liouville equations

The self-adjoint matrix $-iP_0$ has eigenvalues $\lambda_0 = 0$ of multiplicity $d-1$ and $\lambda^\varepsilon_{1,2}(\mathbf{x},\mathbf{k}) = \pm c_\varepsilon(\mathbf{x})|\mathbf{k}|$ and can be diagonalized as

$$-iP_0(\mathbf{x},\mathbf{k}) = \sum_{q=0}^{2} \lambda^\varepsilon_q(\mathbf{x},\mathbf{k})\Pi_q(\mathbf{x},\mathbf{k}), \qquad \text{where} \qquad \sum_{q=0}^{2} \Pi_q(\mathbf{x},\mathbf{k}) = I.$$

The Liouville approximation to the Wigner transform is given by

$$U_\varepsilon(t,\mathbf{x},\mathbf{k}) = \sum_q u^\varepsilon_q(t,\mathbf{x},\mathbf{k})\Pi_q(\mathbf{k}),$$

where the coefficients u^ε_q solve the Liouville equation

$$\begin{aligned} &\frac{\partial u^\varepsilon_q}{\partial t} + \nabla_{\mathbf{k}}\lambda^\varepsilon_q \cdot \nabla_{\mathbf{x}} u^\varepsilon_q - \nabla_{\mathbf{x}}\lambda^\varepsilon_q \cdot \nabla_{\mathbf{k}} u^\varepsilon_q = 0 \\ &u^\varepsilon_q(0,\mathbf{x},\mathbf{k}) = \mathrm{Tr}\Pi_q W_0(\mathbf{x},\mathbf{k})\Pi_q \end{aligned}$$

Here, the coefficients λ^ε_q depend on $\delta(\varepsilon)$ and W_0 is chosen *independent* of ε.

Approximation of W_ε by Liouville equation

Theorem. Let $\rho_\varepsilon(\mathbf{x}) = \rho_0 + \sqrt{\delta}\rho_1(\frac{\mathbf{x}}{\delta})$ and $\kappa_\varepsilon(\mathbf{x}) = \kappa_0 + \sqrt{\delta}\kappa_1(\frac{\mathbf{x}}{\delta})$, with all terms sufficiently smooth. Then we have

$$\|W_\varepsilon(t,\mathbf{x},\mathbf{k}) - U_\varepsilon(t,\mathbf{x},\mathbf{k})\|_2 \le C\frac{\varepsilon}{\delta^m}\exp(\frac{Ct}{\delta^{3/2}})\|W_0\|_{H^3} + \|W_\varepsilon^0 - W_0\|_{L^2},$$

for some m independent of ε.

In other words, assuming that W_ε^0 converges strongly to W_0 and that $\delta(\varepsilon) \to 0$ as $\varepsilon \to 0$ with the constraint $\delta(\varepsilon) \gg |\ln\varepsilon|^{-2/3+\eta}$, then the difference $\|W_\varepsilon(t,\mathbf{x},\mathbf{k}) - U_\varepsilon(t,\mathbf{x},\mathbf{k})\|_{L^2} \to 0$ uniformly on final intervals $t \in (0,T)$.

The convergence is uniform in the realization of the random medium (the statistics of ρ_1 and κ_1 have not been defined yet). So we *safely replace the analysis* of W_ε by that of U_ε, the solution of a Liouville equation with random coefficients.

Analysis of the random Liouville equation

The Liouville equation is of the form

$$\frac{\partial u_\varepsilon}{\partial t} + \Big(c_0 + \sqrt{\delta} c_1(\frac{\mathbf{x}}{\delta})\Big)\hat{\mathbf{k}} \cdot \nabla_{\mathbf{x}} u_\varepsilon - \frac{|\mathbf{k}|}{\sqrt{\delta}} \nabla_{\mathbf{x}} c_1(\frac{\mathbf{x}}{\delta}) \cdot \nabla_{\mathbf{k}} u_\varepsilon = 0,$$
$$u_\varepsilon(0, \mathbf{x}, \mathbf{k}) = u_0(\mathbf{x}, \mathbf{k}).$$

Its solution is given by $u_\varepsilon(t, \mathbf{x}, \mathbf{k}) = u_0(\mathbf{X}(t), \mathbf{K}(t))$, where

$$-\frac{d\mathbf{X}}{dt} = \Big(c_0 + \sqrt{\delta} c_1(\frac{\mathbf{X}(t)}{\delta})\Big)\hat{\mathbf{K}}, \qquad \mathbf{X}(0) = \mathbf{x},$$
$$-\frac{d\mathbf{K}}{dt} = -\frac{|\mathbf{K}(t)|}{\sqrt{\delta}} \nabla_{\mathbf{x}} c_1(\frac{\mathbf{X}(t)}{\delta}), \qquad \mathbf{K}(0) = \mathbf{k}.$$

Decorrelation of nearby particles

Let us assume that two particles satisfy the system for $j = 1, 2$,

$$\frac{d\mathbf{X}_j^{(\delta)}(t)}{dt} = \Big(c_0 + \sqrt{\delta}c_1(\frac{\mathbf{X}_j^{(\delta)}(t)}{\delta})\Big)\hat{\mathbf{K}}_j^{(\delta)}(t), \quad \mathbf{X}_j^{(\delta)}(0) = \mathbf{x}_j$$
$$\frac{d\mathbf{K}_j^{(\delta)}(t)}{dt} = \frac{1}{\sqrt{\delta}}\nabla_{\mathbf{x}} c_1(\frac{\mathbf{X}_j^{(\delta)}(t)}{\delta})|\mathbf{K}_j^{(\delta)}(t)|, \quad \mathbf{K}_j^{(\delta)}(0) = \mathbf{k}_j.$$

Under suitable mixing conditions for c_1 and for $\mathbf{k}_1 \neq \mathbf{k}_2$, the laws of the processes $(\mathbf{K}_1^{(\delta)}, \mathbf{X}_1^{(\delta)}, \mathbf{K}_2^{(\delta)}, \mathbf{X}_2^{(\delta)})$ converge weakly as $\delta \to 0$ to the law of $(\mathbf{K}_1, \mathbf{X}_1, \mathbf{K}_2, \mathbf{X}_2)$, where $\mathbf{X}_j(t) = \mathbf{x}_j + c_0 \int_0^t \hat{\mathbf{K}}_j(s)ds, \quad j = 1, 2$, and where $\mathbf{k}_j(\cdot)$, $j = 1, 2$ are independent symmetric diffusions in $\mathbb{R}^d \setminus \{\mathbf{0}\}$ starting at $\mathbf{k}_j$, $j = 1, 2$ correspondingly with common generator

$$\mathcal{L}F(\mathbf{k}) = \sum_{p,q=1}^{d} |\mathbf{k}|^2 D_{p,q}(\hat{\mathbf{k}})\partial^2_{k_p,k_q}F(\mathbf{k}) + \sum_{p=1}^{d} |\mathbf{k}|E_p(\hat{\mathbf{k}})\partial_{k_p}F(\mathbf{k}).$$

Stability of the Wigner Transform

We deduce from the previous result that

$$\mathbb{E}\{u_\varepsilon(t,\mathbf{x},\mathbf{k})\} \to F(t,\mathbf{x},\mathbf{k}) \qquad \text{weakly as} \qquad \delta(\varepsilon)\to 0,$$

where F satisfies the following Fokker-Planck equation

$$\frac{\partial F}{\partial t} + c_0 \hat{\mathbf{k}}\cdot\nabla_{\mathbf{x}} F - \mathcal{L}F = 0.$$

Moreover, we obtain the stability result

$$\mathbb{E}\left\{\int \left|\left\langle u_\varepsilon(T,\mathbf{x}_0,\mathbf{k}) - F(T,\mathbf{x}_0,\mathbf{k}), \lambda(\mathbf{k})\right\rangle\right|^2 d\mathbf{x}_0\right\} \to 0 \qquad \text{as} \qquad \delta(\varepsilon)\to 0,$$

which implies that u_ε converges in probability to the deterministic solution F. This in turn implies the stability of the refocused signal $\mathbf{u}^B$.

Summary of radiative transfer models

We have obtained several transport models of the form

$$\frac{\partial a}{\partial t} + c_0 \hat{\mathbf{k}} \cdot \nabla_{\mathbf{x}} a + \mathcal{S} a = 0,$$

where the scattering operator $\mathcal{S}$ is given respectively by

$$\begin{aligned}
&\text{Radiative Transfer:} & \mathcal{S}a &= \int_{\mathbb{R}^d} \hat{R}(\mathbf{p}-\mathbf{k})(a(\mathbf{k})-a(\mathbf{p}))\delta\Big(c_0|\mathbf{p}|-c_0|\mathbf{k}|\Big)d\mathbf{k}\\
&\text{Paraxial:} & \mathcal{S}a &= \int_{\mathbb{R}^{d-1}} \hat{R}\Big(\frac{|\mathbf{p}'|^2-|\mathbf{k}'|^2}{2}, \mathbf{p}'-\mathbf{k}'\Big)(a(\mathbf{k}')-a(\mathbf{p}'))d\mathbf{k}'\\
&\text{Itô-Schrödinger:} & \mathcal{S}a &= \int_{\mathbb{R}^{d-1}} \hat{R}(0, \mathbf{p}'-\mathbf{k}')(a(\mathbf{k}')-a(\mathbf{p}'))d\mathbf{k}'\\
&\text{Fokker-Planck:} & \mathcal{S}a &= -D(|\mathbf{k}|)\Delta_{\hat{\mathbf{k}}} a.
\end{aligned}$$

Note that Radiative Transfer and Fokker-Planck admit a diffusion limit for small mean free paths. This can be arranged for the paraxial approximation when $\hat{R}(t,\cdot) \approx \delta(t)\hat{R}'(\cdot)$, but *not* for Itô-Schrödinger.

Summary of Kinetic models for Time Reversal

• We have a theory to express the high frequency limit of the refocused signal in Time Reversal experiments using a Wigner transform. In the scalar case, this expression is

$$\hat{u}^B(\mathbf{p};\mathbf{x}_0) = W(T,\mathbf{x}_0,\mathbf{p})\hat{S}(\mathbf{p};\mathbf{x}_0).$$

The filter can also be generalized to changing environments.

• In certain cases, we can rigorously characterize the high frequency limit of the Wigner transform and if possible (and true) obtain its stability. This has been done for the parabolic approximation and the Itô Schrödinger approximation, and in the random Liouville regime, where high frequency waves are approximated by particles propagating in random media.

Outline

1. Time Reversal in random media and kinetic models

2. Statistical stability and rigorous theories

3. **Validity of Radiative Transfer Models**

4. Applications to Detection and Imaging

Time reversal in changing media

Consider two media with compressibility fluctuations given by $\hat{\kappa}_2(\mathbf{x},\mathbf{k}) = \phi(\mathbf{x}) e^{i\boldsymbol{\tau}\cdot\mathbf{k}} \hat{\kappa}_1(\mathbf{x},\mathbf{k})$. For instance $\phi(\mathbf{x})$ corresponds to a change in the amplitude of the fluctuations at the macroscopic scale $\mathbf{x}$ and $\boldsymbol{\tau}$ corresponds to a spatial shift in the domain before back-propagation.

In the diffusive regime, the back-propagated signal takes the form

$$\hat{\mathbf{u}}^B(\mathbf{k};\mathbf{x}_0) = \left[\begin{pmatrix} \sin(\Pi_s T)\sqrt{\dfrac{\kappa_0}{\rho}} i\hat{\mathbf{k}} \\ \cos(\Pi_s T) \end{pmatrix} \hat{p}_0(\mathbf{k}) + \begin{pmatrix} \cos(\Pi_s T) i\hat{\mathbf{k}} \\ -\sin(\Pi_s T)\sqrt{\dfrac{\rho}{\kappa_0}} \end{pmatrix} |\mathbf{k}|\hat{\varphi}(\mathbf{k}) \right]$$
$$\times\ e^{-i\boldsymbol{\tau}\cdot\mathbf{k}} \ \frac{\sin|\boldsymbol{\tau}||\mathbf{k}|}{|\boldsymbol{\tau}||\mathbf{k}|} \ e^{-\Sigma\psi^2 T/2} \ a(T,\mathbf{x}_0,|\mathbf{k}|).$$

This is to be compared to the case where $\Pi_s = \psi = |\boldsymbol{\tau}| = 0$ when the medium remains the same during the forward and backward propagations.

2D Numerical simulations

In two space dimensions and in the case of periodic media with large distances of propagation relative to the size of the box, the filter is asymptotically given by

$$F(\psi, |\boldsymbol{\tau}|, |\mathbf{k}|, T, L, k_{\text{max}}, \kappa) = \bar{a}\, J_0(|\boldsymbol{\tau}||\mathbf{k}|)\, \cos(2\psi\Pi_0 T)\, e^{-\frac{\Sigma}{2}\psi^2 T}.$$

It should be compared to the numerical simulation

$$F_{\text{data}} = \frac{(p^B(\mathbf{x}+\boldsymbol{\tau}), p_0(\mathbf{x}))}{\|p_0(\mathbf{x})\|^2}.$$

We consider some simulations with varying $|\boldsymbol{\tau}|$ (shifting medium).

2D Numerical simulations (II)

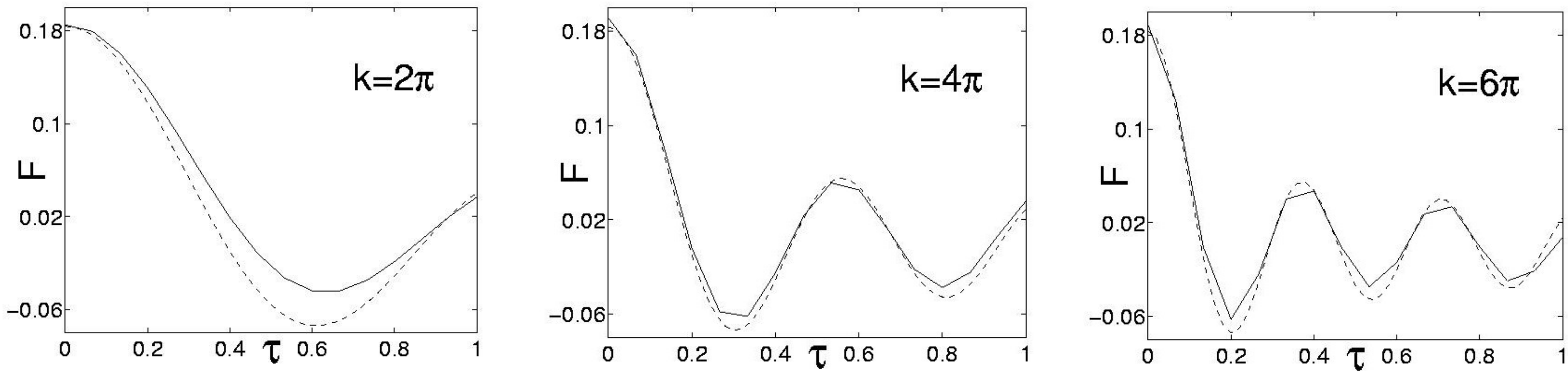

Comparison of F_{data} (solid lines) and the theoretical prediction F (dashed lines) as a function of τ with $\psi = 0$. Periodic box of size $L = 20$, propagation time $T = 200$, number of modes in power spectrum: 50.

Duke experimental setting

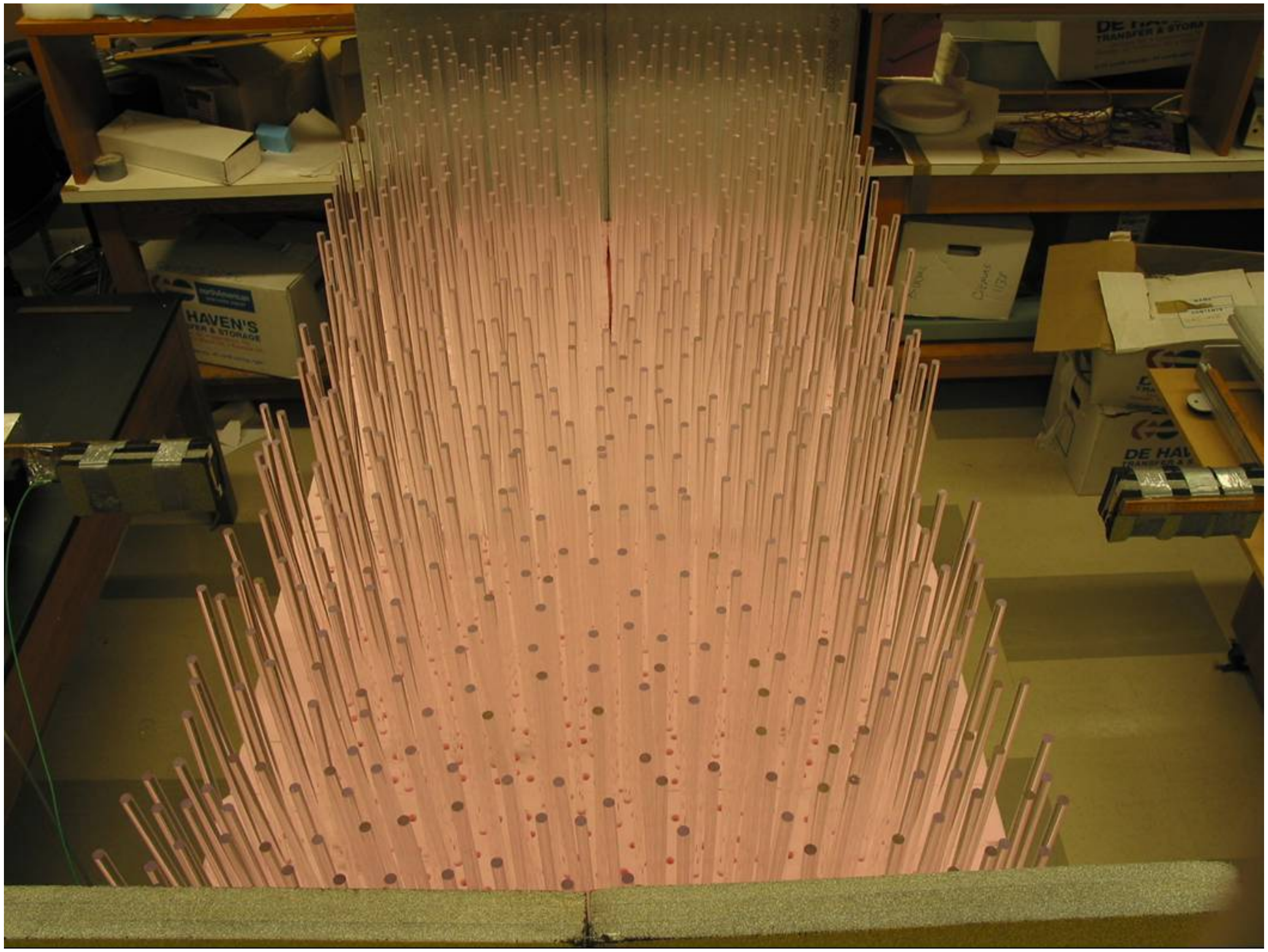

Spatial shift before backpropagation

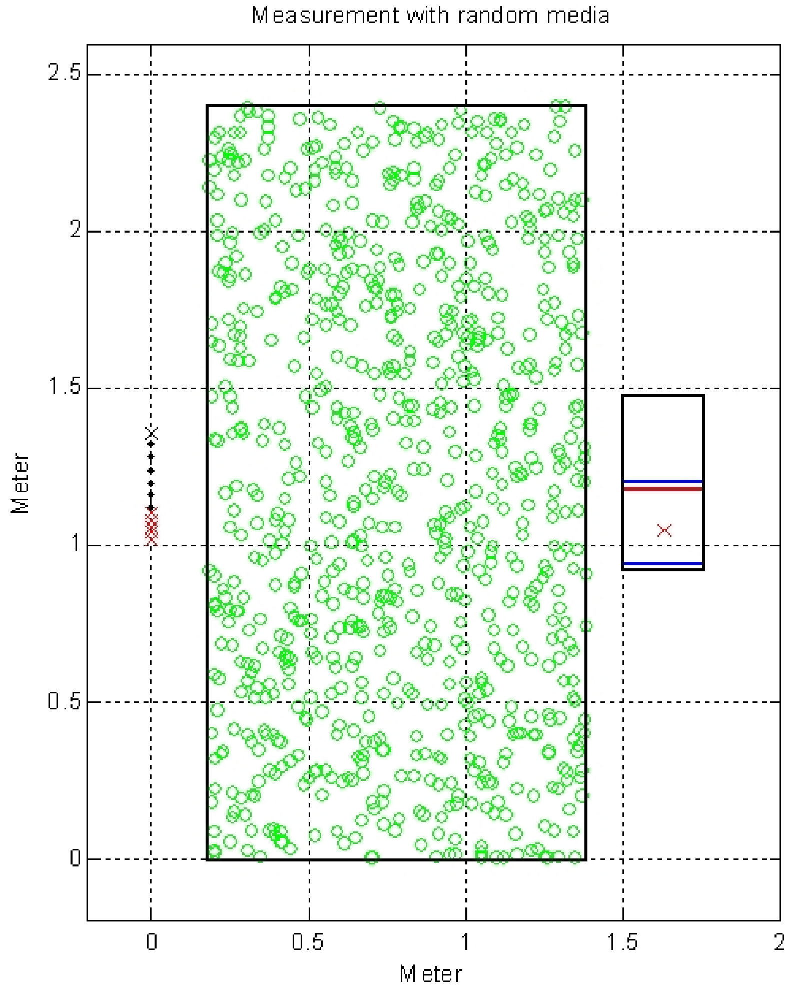

Back-propagated signal

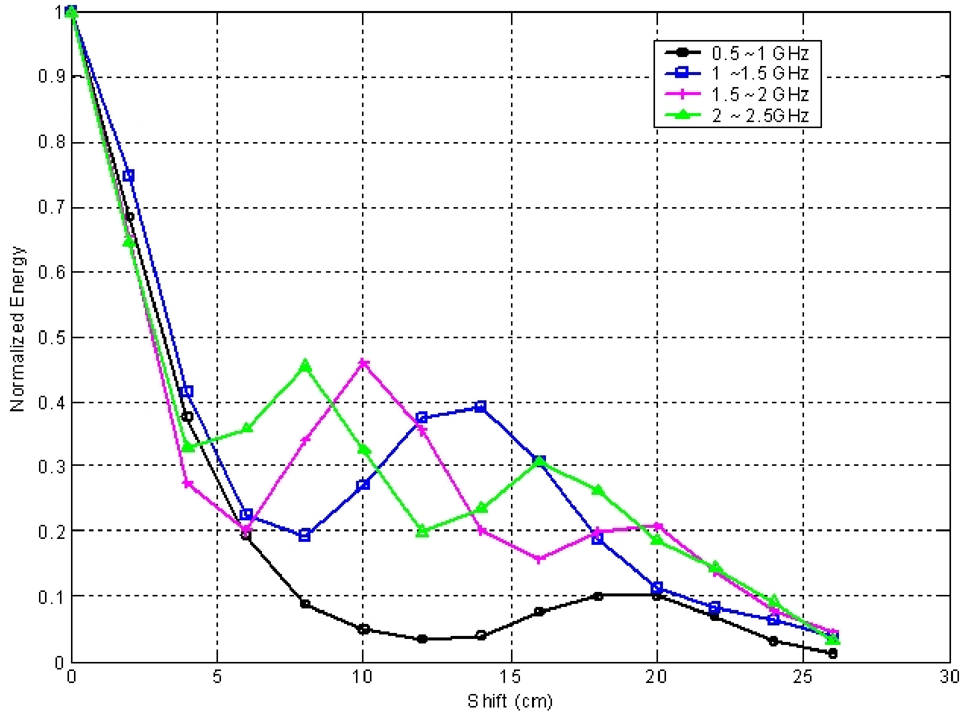

Back-propgated signal as a function of spatial shift for several frequencies. The minimum of the back-propagated signal exactly occurs where it is predicted by the two-dimensional theory.

Numerical validation of radiative transfer

Wave propagation in heterogeneous media may sometimes be difficult to control in real experiments. Numerical simulations offer an interesting complement to physical experiments.

In order to be relevant the simulations need to consider spatial domains that are much larger than the typical wavelength in the system. This requires us to use multi-processor architectures and parallelized codes.

We have developed such a computational tool to solve acoustic waves (easily extendible to micro-waves) in the time domain.

Details of the wave (microscopic) code.

The codes solves a discrete version (centered second-order discretization in space and time) of the following acoustic wave system of equation

$$\frac{\partial \mathbf{v}}{\partial t} + \rho^{-1}(\mathbf{x})\nabla p = 0,$$
$$\frac{\partial p}{\partial t} + \kappa^{-1}(\mathbf{x})\nabla \cdot \mathbf{v} = 0.$$

The domain is surrounded by a perfectly matched layer (PML) method so that outgoing waves are not reflected at the domain boundary. The (random) physical coefficients $\rho(\mathbf{x})$ and $\kappa(\mathbf{x})$ are carefully chosen to verify prescribed statistical properties.

The FDFT (Finite difference forward in time) method has been parallelized by using the software PETSc developed at Argonne. Forward calculations for $T = 1500$ (typical times necessary to validate the diffusive model; for $\lambda = 1$ and average sound speed $c_0 = 1$) require 3-4 days of calculations.

Details of the macroscopic codes.

In both the direct and time reversal measurements, the data are the macroscopic energy densities

$$\mathcal{E}(t,\mathbf{x}) = \frac{1}{2}\Big(\rho(\mathbf{x})|\mathbf{v}|^2(t,\mathbf{x}) + \kappa(\mathbf{x})p^2(t,\mathbf{x})\Big).$$

We consider two macroscopic models for $\mathcal{E}$: a radiative transfer equation and a diffusion equation. The radiative transfer equation is solved by a Monte Carlo method (requiring in excess of $50M$ particles to achieve a reasonable accuracy even with good variance reduction technique conditioning particles on hitting the inclusion). The diffusion equation is solved by the finite element method.

A typical configuration for the wave solver

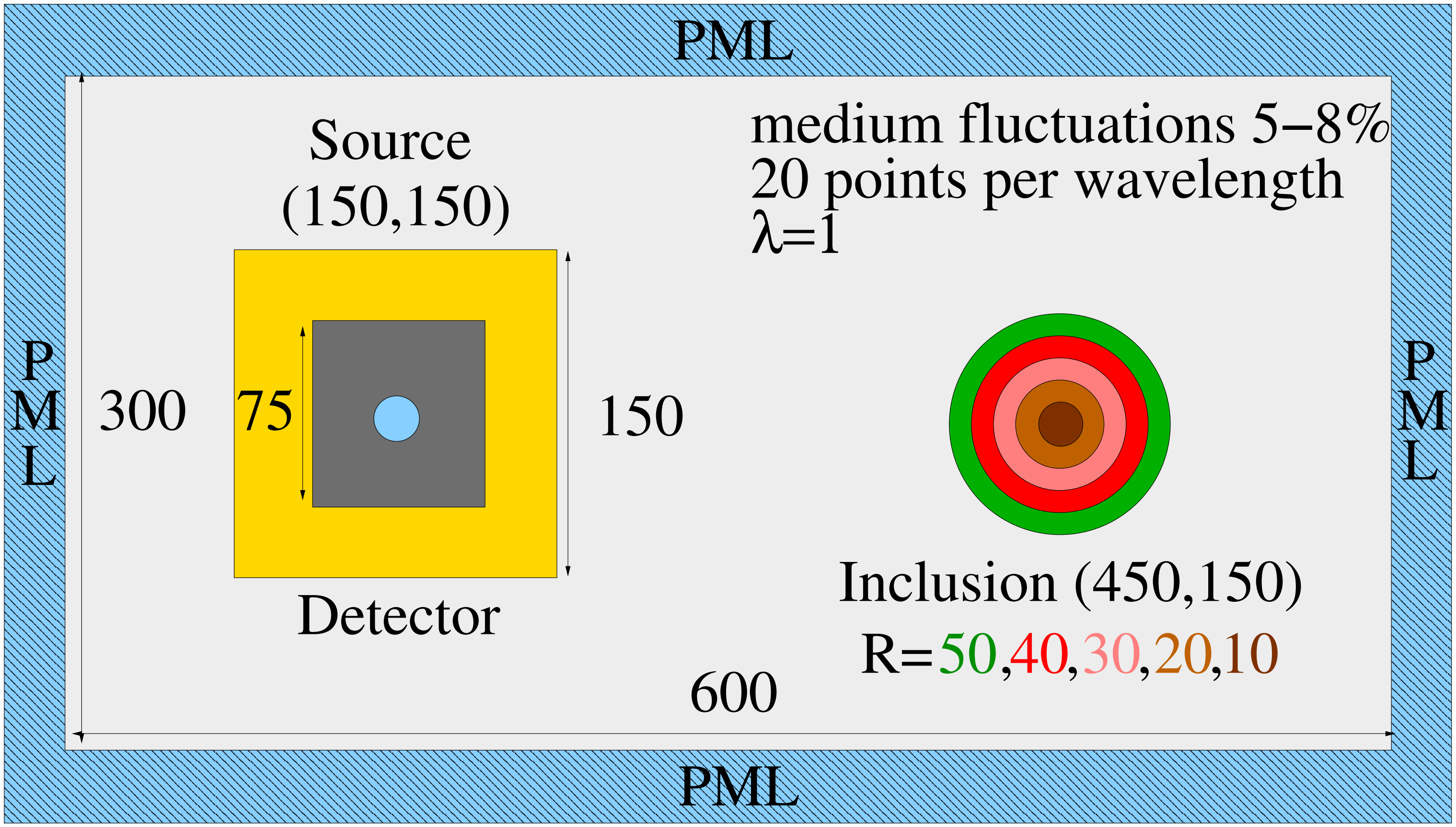

The domain size is roughly $20,000 \times 10,000 = 200M$ nodes

Wave-Transport-diffusion comparison

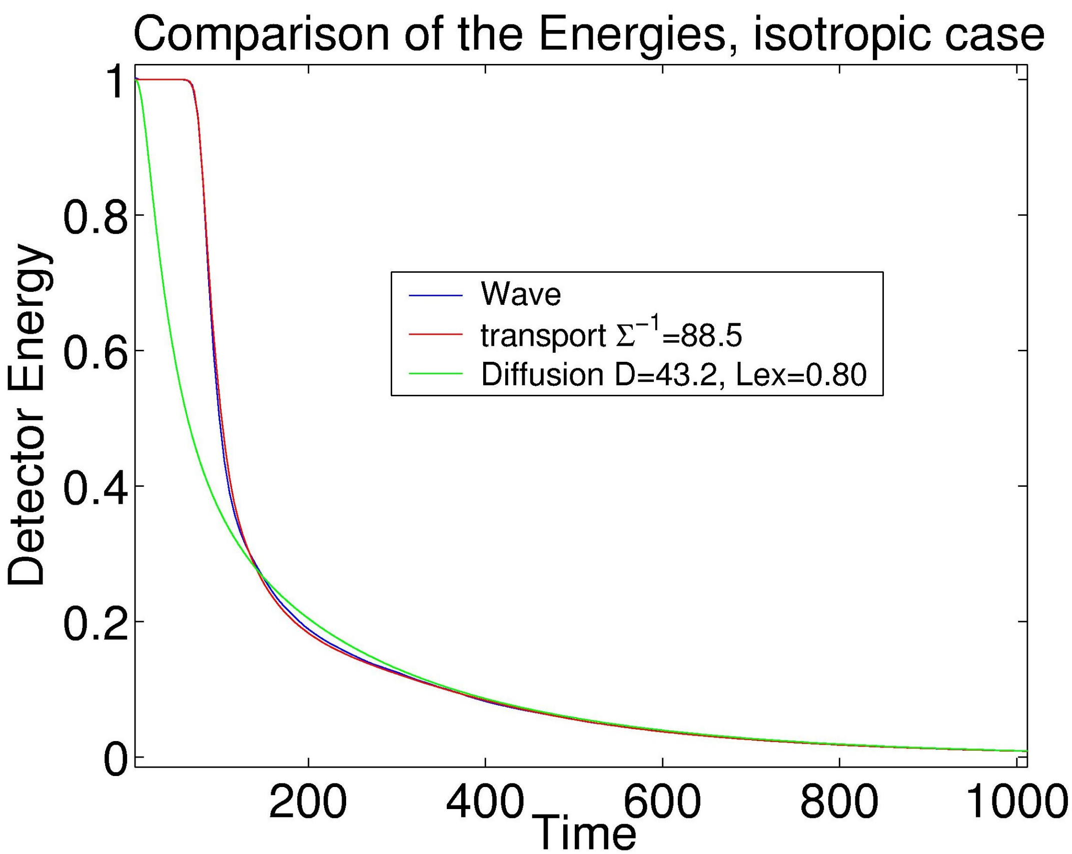

Experiment with isotropic scattering ($\hat{R} \equiv 1$ for this frequency; the source term is a localized Bessel function). The best transport fit is obtained for $\Sigma^{-1}_{\text{num}} = 88.5$ versus $\Sigma^{-1}_{\text{th}} = 83.00$. The best fit for the diffusion coefficient and the extrapolation length are $D_{\text{num}} = 43.2$ and $L_{\text{ex}} = 0.80$ versus $D_{\text{th}} = (2\Sigma)^{-1} = 41.5$ and $L_{\text{th}} = 0.81$.

Averaged energy densities on detector as a function of time.

Effect of void inclusion

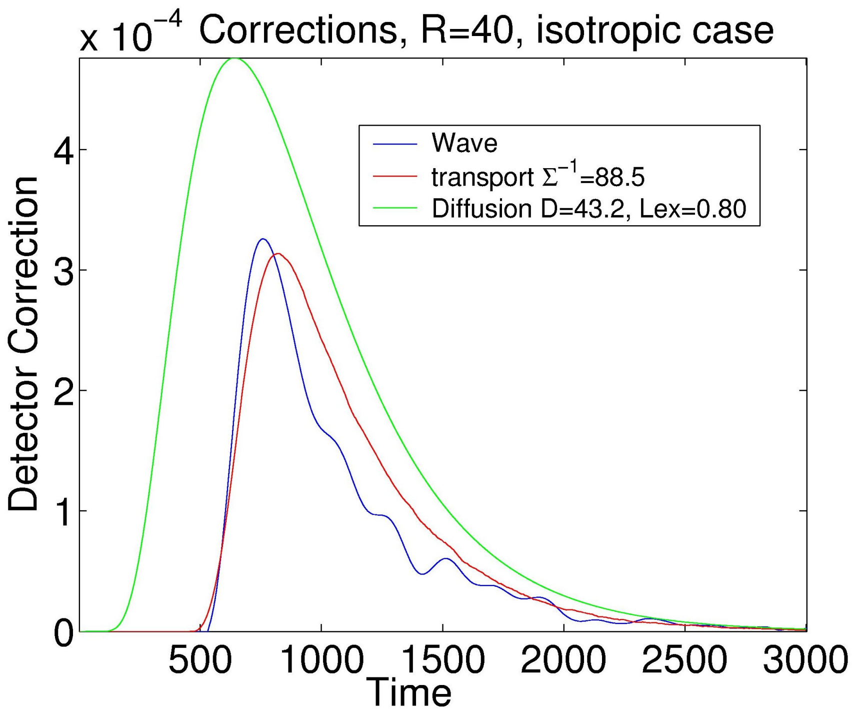

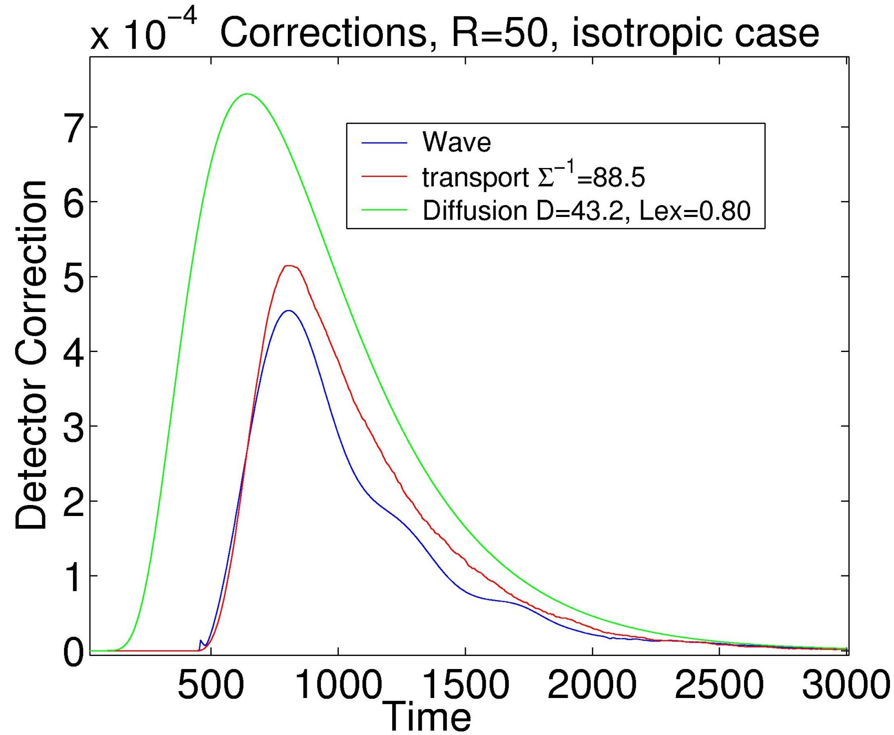

Correction (w.r.t. solution without inclusion) generated by a void inclusion, where the random fluctuations are suppressed. Left, radius of 40. Right, radius of 50. Transport and diffusion generated by best energy fit. The diffusion fit is valid only for very long times, whereas transport performs extremely well.

Effect of increased randomness

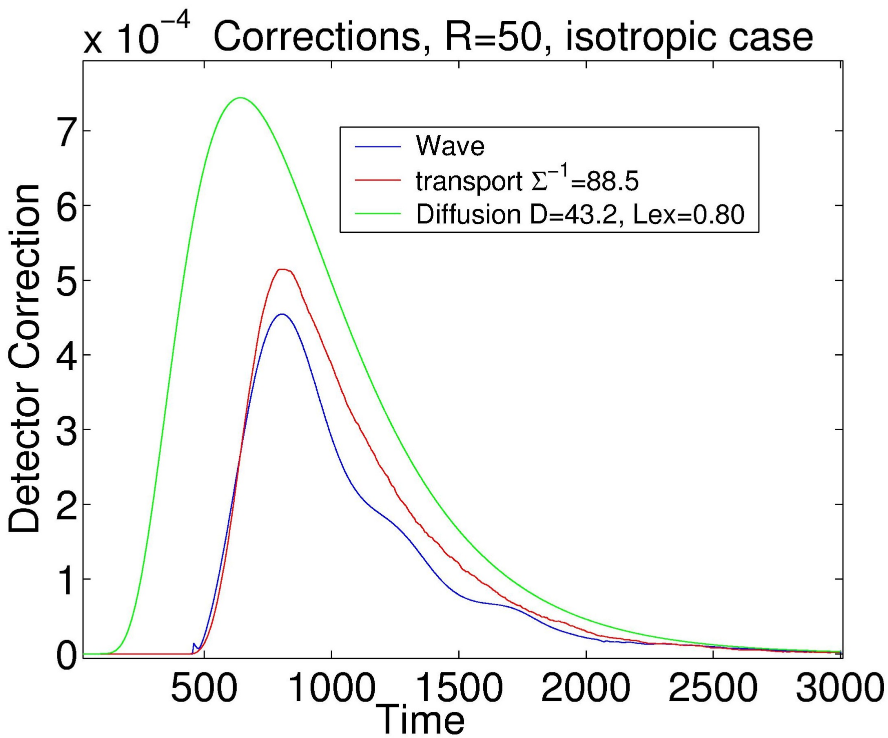

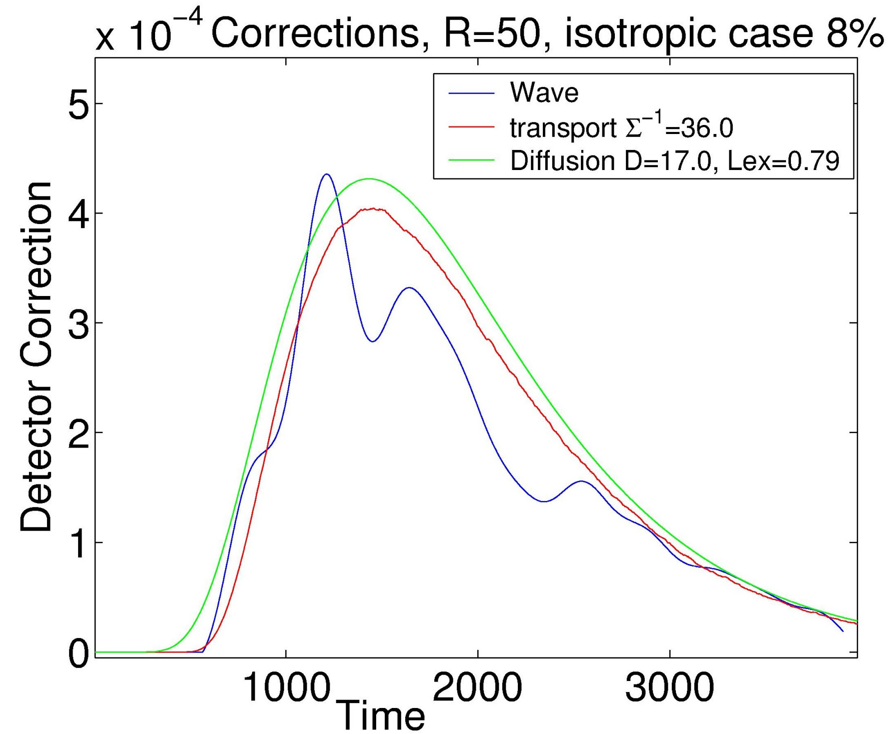

Correction generated by an inclusion of radius $R = 50$ where the random fluctuations are suppressed. Left: 5% RMS. Right: 8% RMS. Transport and diffusion generated by best energy fit. The diffusion fit is now much more accurate.

Effect of perfectly reflecting inclusion

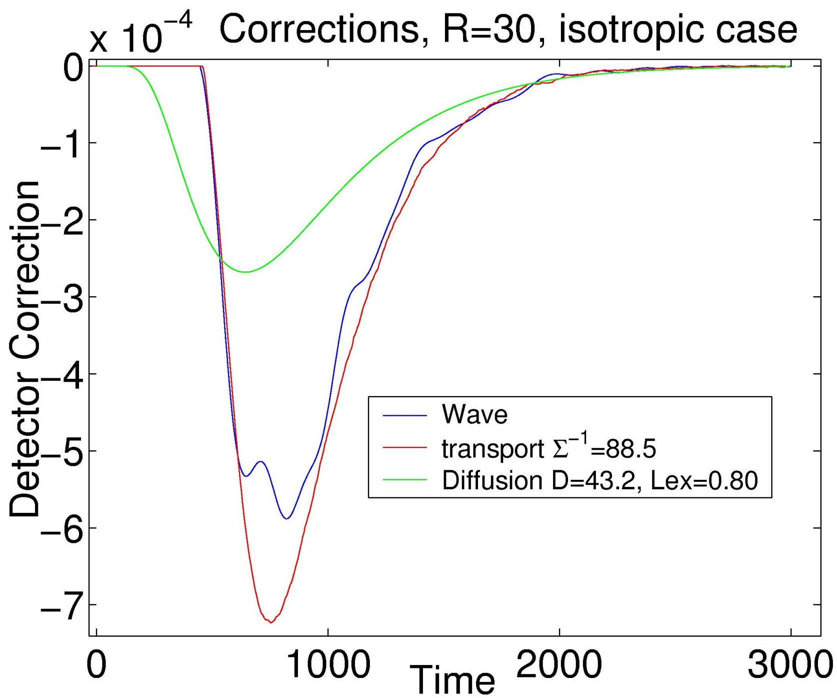

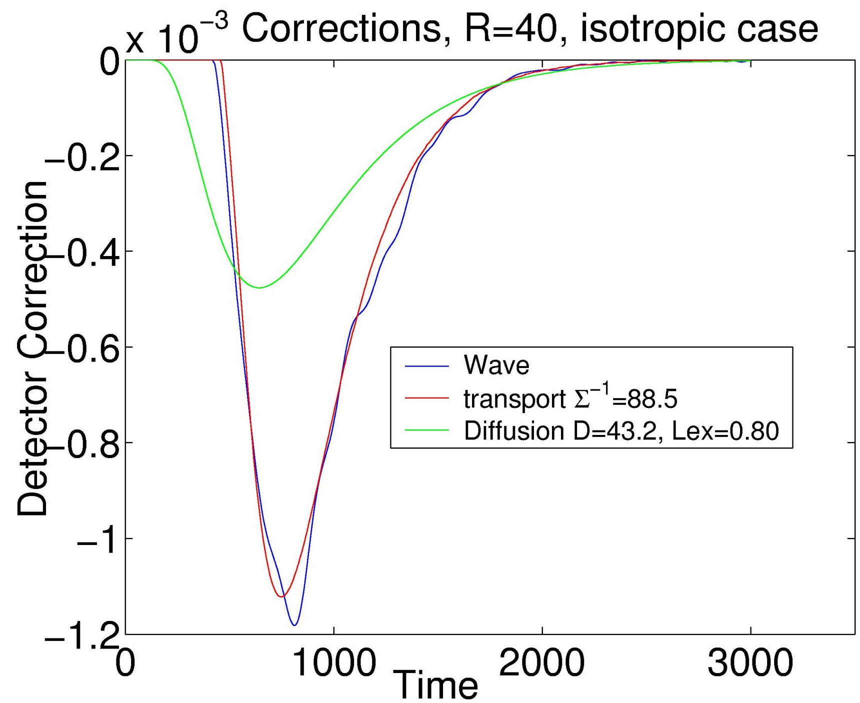

Correction generated by a perfectly reflecting inclusion (specular reflection for transport and Neumann conditions for diffusion). Left, radius of 30. Right, radius of 40. Transport and diffusion generated by best energy fit. Still very good agreement between wave and transport simulations.

Effect of a (4 times) smaller detector

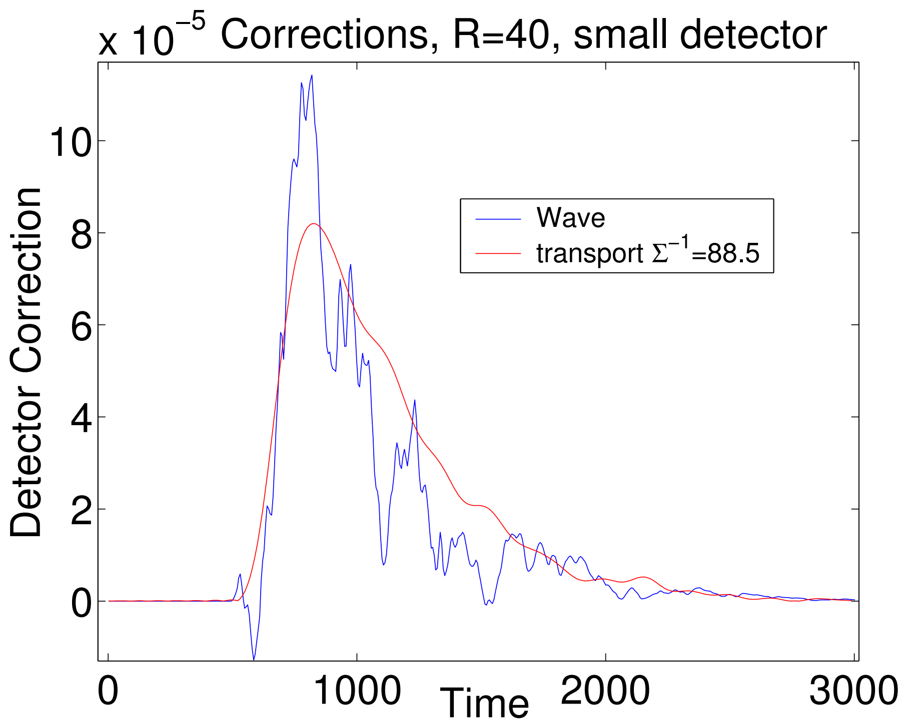

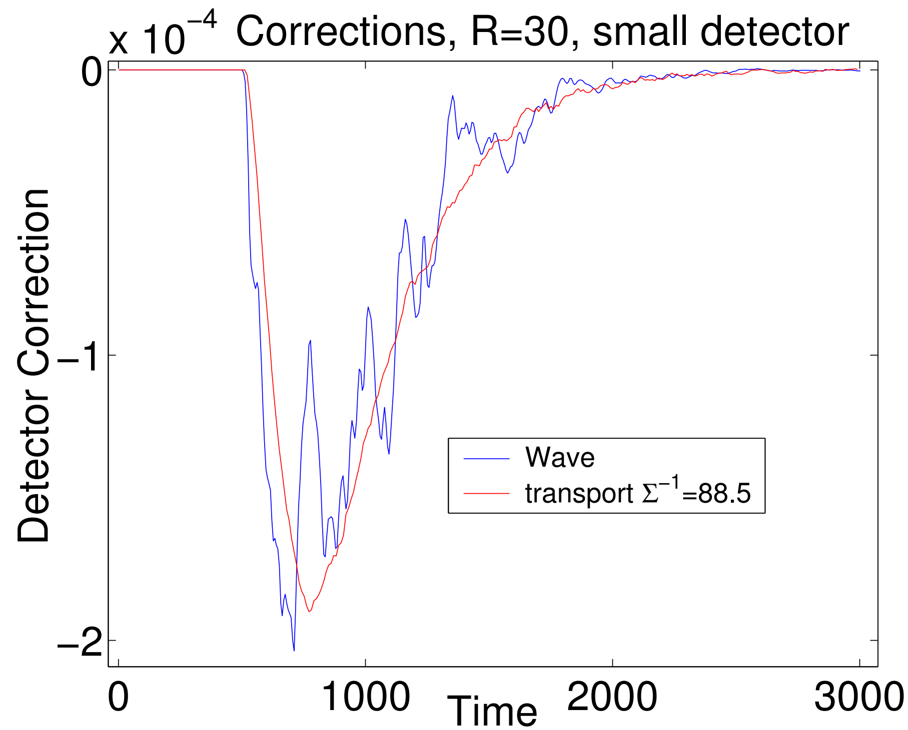

Comparison of wave and transport predictions. Isotropic medium with 5% RMS. Left: void inclusion with $R = 40$; Right: reflecting inclusion with $R = 30$.

Effect of a smaller inclusion

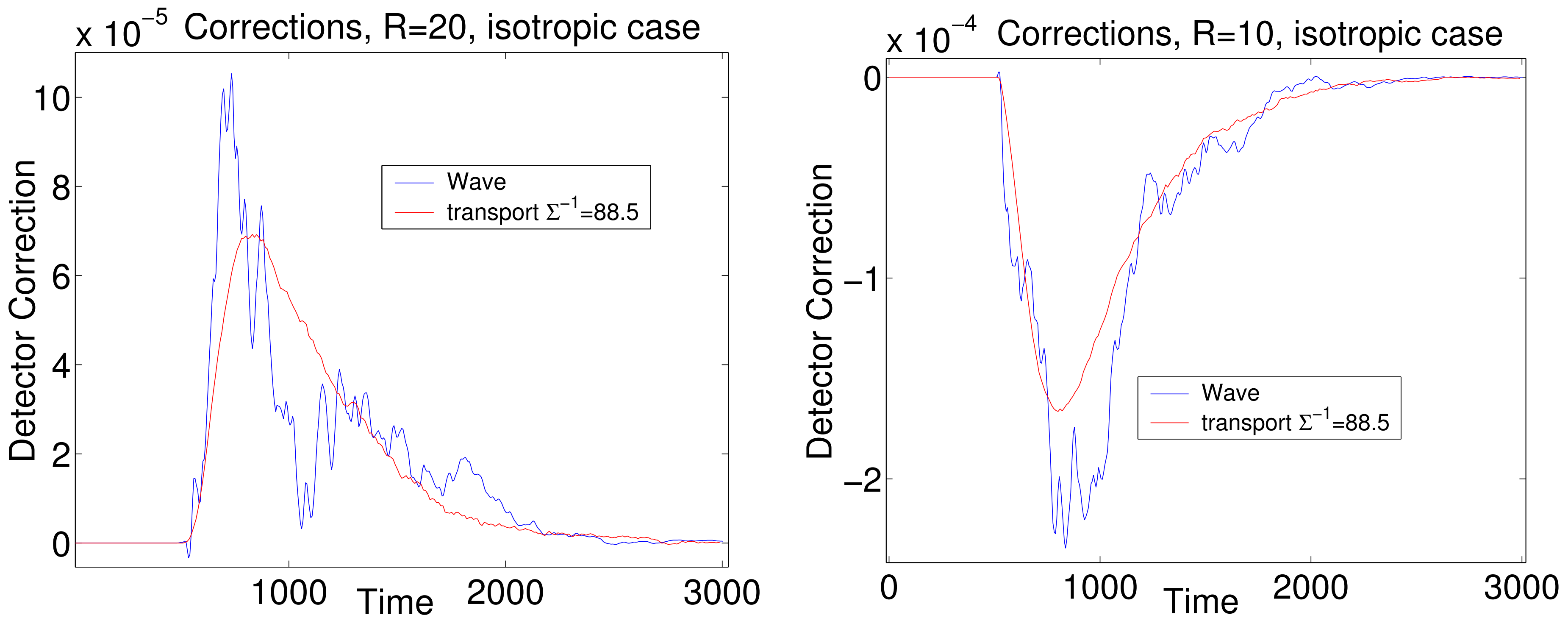

Comparison of wave and transport predictions with large detector. Isotropic medium with 5% RMS. Left: void inclusion with $R = 20$; Right: reflecting inclusion with $R = 10$. Conclusion: Radiative transfer is statistically stable when sufficient averaging takes place.

Outline

1. Time Reversal in random media and kinetic models

2. Statistical stability and rigorous theories

3. Validity of Radiative Transfer Models

4. **Applications to Detection and Imaging**

Experimental setting; forward stage

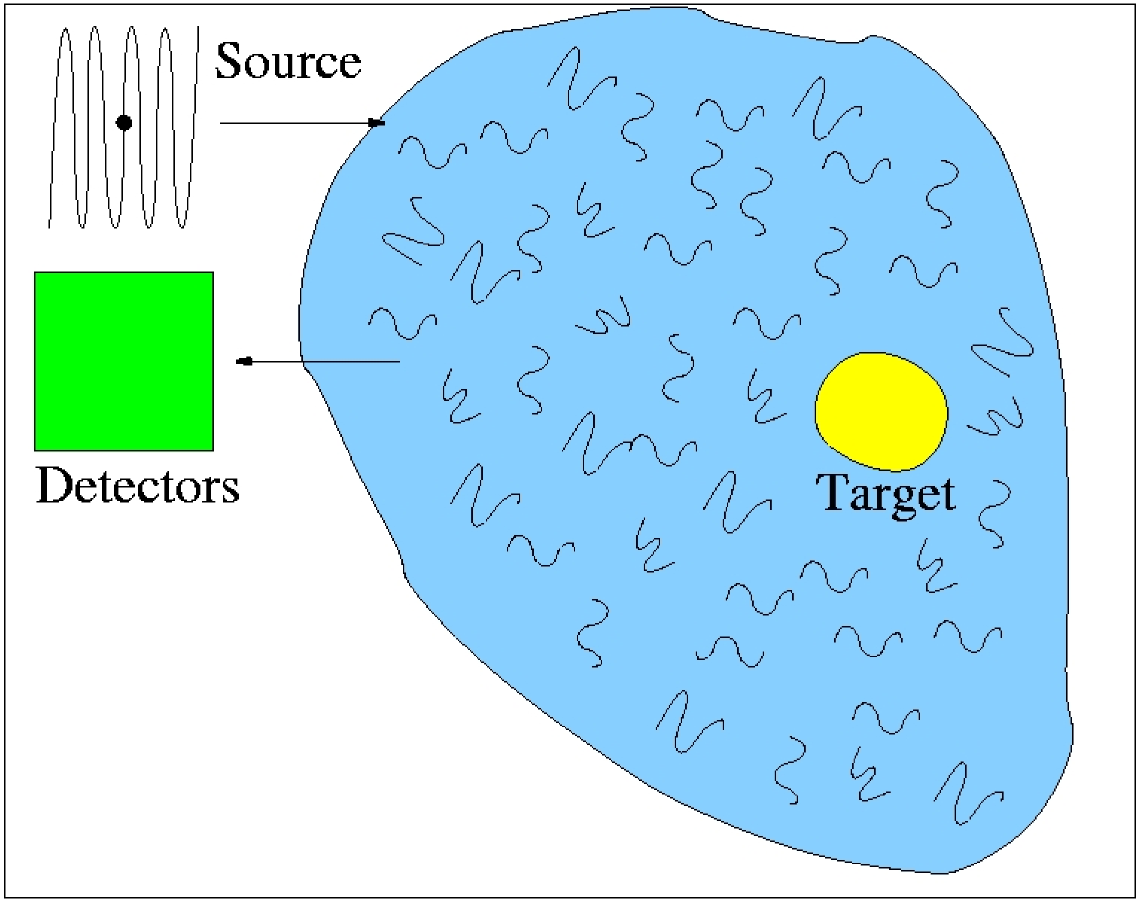

Experimental setting; backward stage

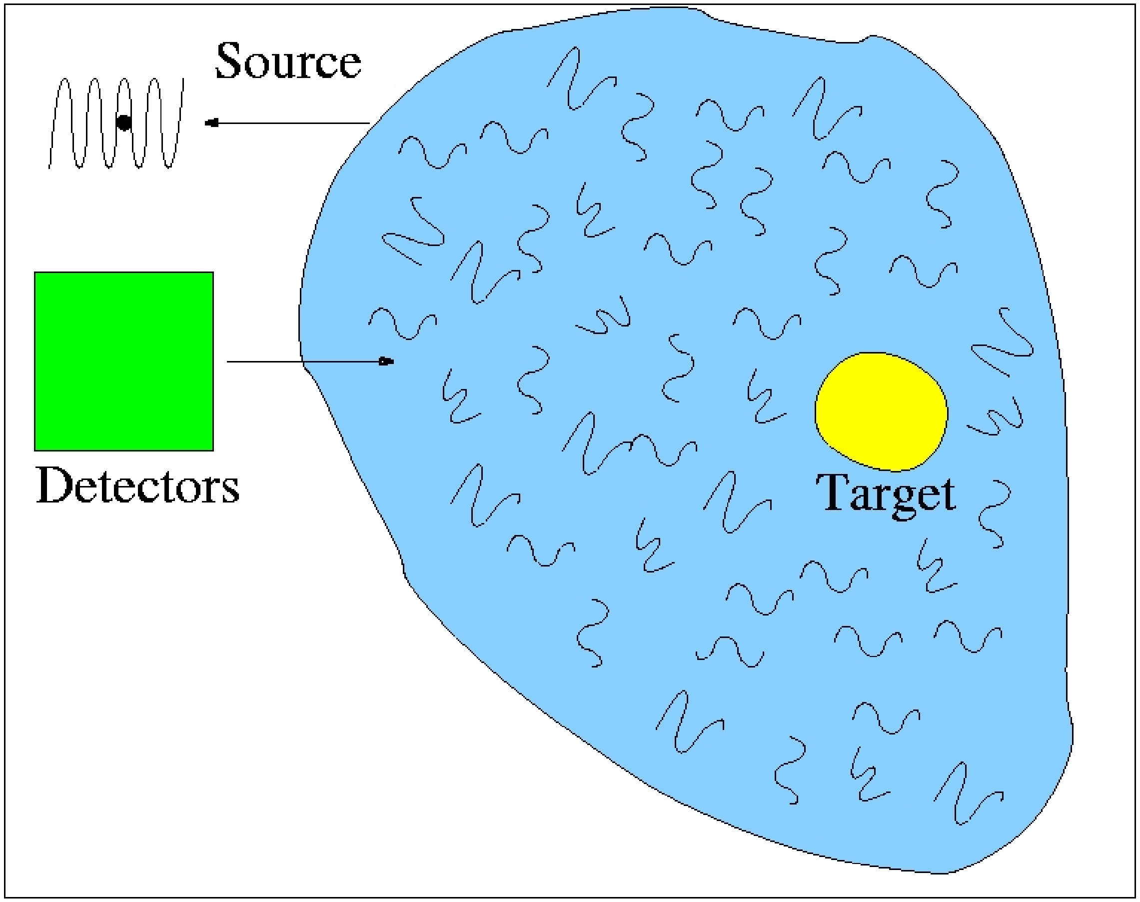

Modeling the inclusion

The detection and imaging of buried inclusions (which are large compared to the wavelength) is done as follows. We model the inclusion as a variation in the kinetic parameters of the radiative transfer equation that models the wave energy density.

The objective is to reconstruct these kinetic parameters from wave energy measurements at the boundary of a domain. This is severely ill-posed problem (in the sense that the reconstruction amplifies noise drastically). Because the inclusion is assumed to be of small volume (at the macroscopic scale), further assumptions are possible. We consider asymptotics in the volume of the inclusion, which take the form

$$\delta a^0(t,\mathbf{x},\mathbf{k}) = -|B| \int_0^t G(t-s,\mathbf{x},\mathbf{x}_b,\mathbf{k})\,(Qa^0)(s,\mathbf{x}_b,\mathbf{k})ds + \text{l.o.t.},$$

where a^0 is the unperturbed solution, G the transport Green's function, Q the scattering operator and $|B| \sim R^d$ the inclusion's volume.

Reconstruction of the inclusion

Detection and imaging based on the above asymptotic expansions allow us obtain the inclusion's location and volume:

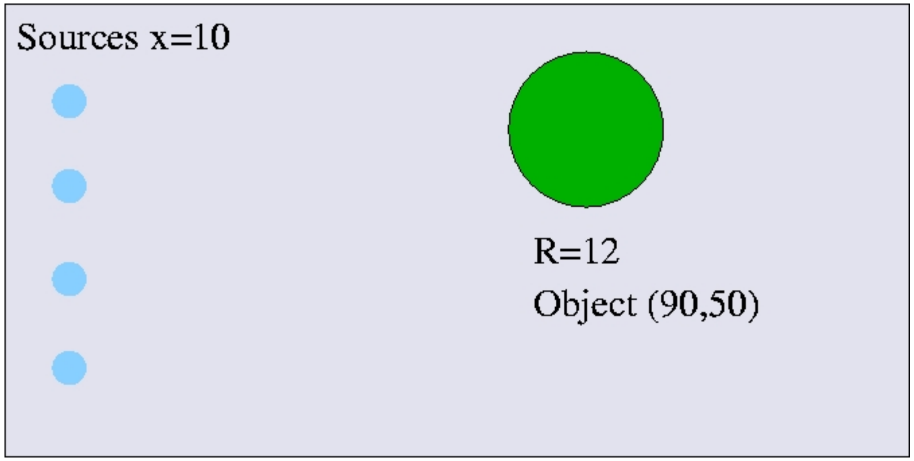

σ_{n}/a_0	error on R (%)	error on x_b	error on y_b
0.25%	12	9.0	3.5
0.5%	25	15	5.0
1%	33	30	10

Very accurate data are required to locate and estimate the inclusion.

TR in Changing media; forward stage

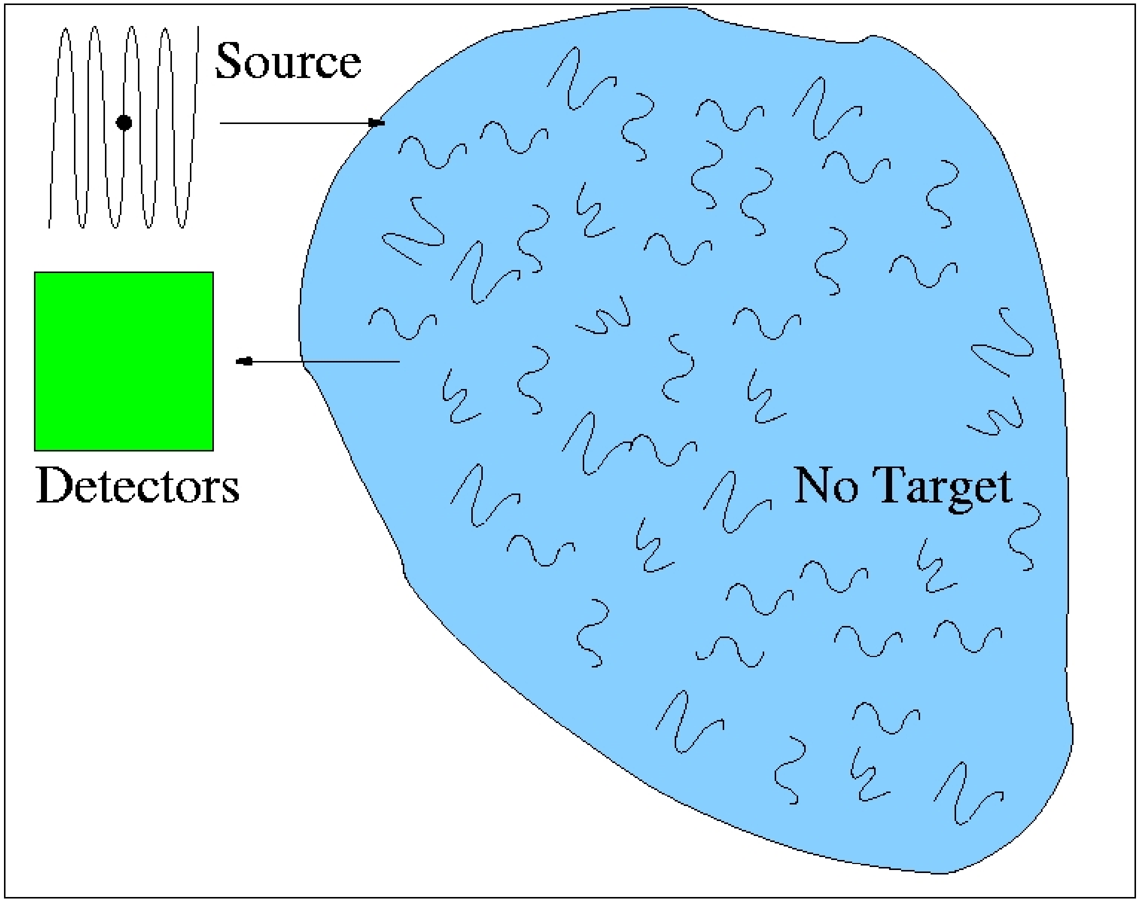

TR in changing media; backward stage

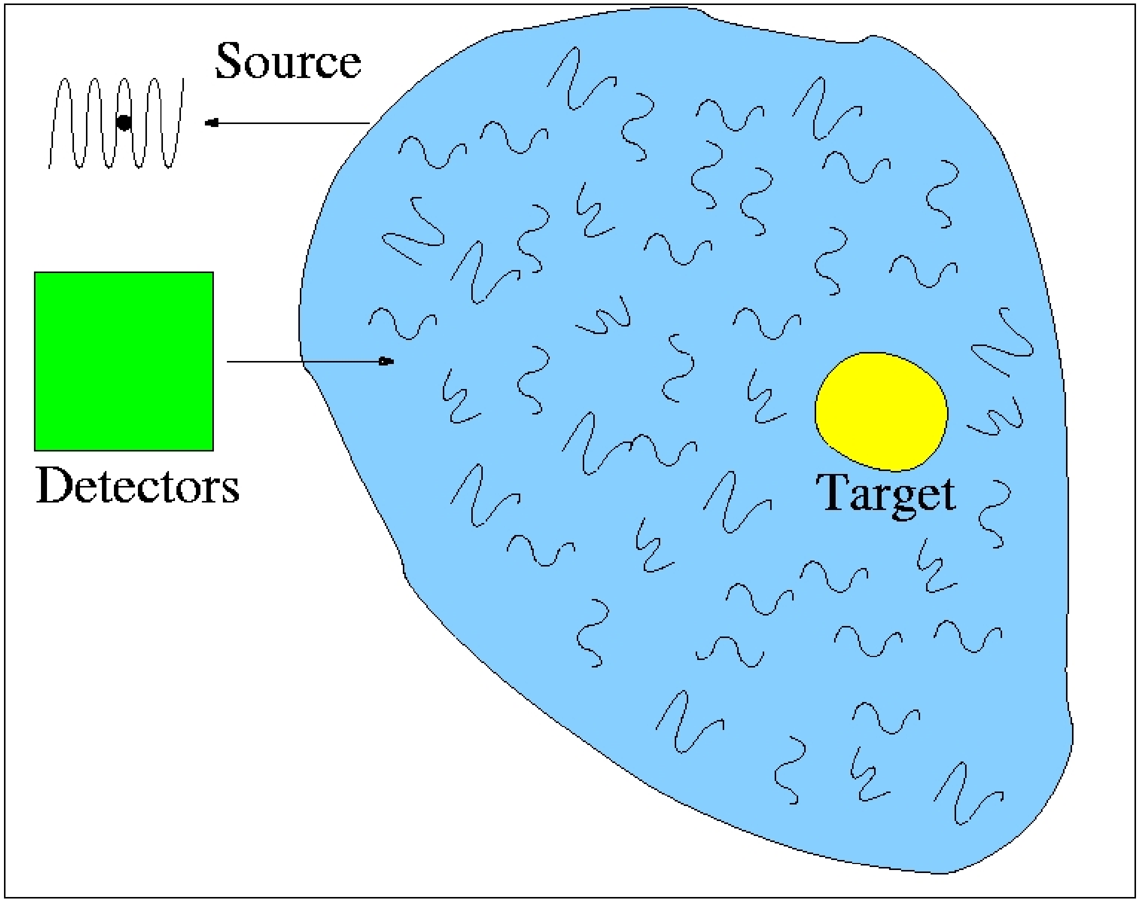

Imaging and changing media

In the diffusive regime, the perturbation caused by a void inclusion is given approximately by

$$\delta u^D(t,\mathbf{x}) = d\pi D_0 R^d \int_0^t \nabla_{\mathbf{x}} u_0(t-s,\mathbf{x}_b)\cdot\nabla_{\mathbf{x}_b} G(s,\mathbf{x},\mathbf{x}_b)ds.$$

Here d is dimension and $G(s,\mathbf{x},\mathbf{x}_b)$ the background Green's function. When we have access to the measured wave field **both** in the presence and in the absence of the inclusion, we can consider the correlation of the two fields. In the diffusive regime, the corresponding perturbation is given by

$$\begin{aligned}
\delta u(t,\mathbf{x}) &= -4\pi R \int_0^t u_0(t-s,\mathbf{x}_b) G(s,\mathbf{x},\mathbf{x}_b) ds + o(R), && d=3 \\
\delta u(t,\mathbf{x}) &= \frac{2\pi}{\ln R} \int_0^t u_0(t-s,\mathbf{x}_b) G(s,\mathbf{x},\mathbf{x}_b) ds + o\Big(\frac{1}{|\ln R|}\Big), && d=2.
\end{aligned}$$

Since $O(R) \gg O(R^3)$ in $d=3$ and $O(|\ln R|^{-1}) \gg O(R^2)$ in $d=2$, it is much easier to detect and image in the presence of differential information.

Can time-reversal experiments help?

Direct energy and time reversal measurements are hampered by two types of noise: background noise n_e and model noise n_m (characterizing the accuracy of the diffusive model). Let U be the direct measurement and F the TR filter measurement. Then we have that (after a few simplifications)

$$\begin{aligned} \delta\tilde{U} &= \delta U + n_m U_0 + n_d \\ \delta\tilde{F} &= \delta F + n_m F_0 + \varepsilon^{d/2} n_d; \quad (d \text{ is dimension}). \end{aligned}$$

Thus both types of measurements are equally affected by the model noise. However, because background noise does not refocus at the source location, it is strongly attenuated in the TR experiment.

In practice, direct measurements are very faint and thus even very small background noise renders the detection impossible. This is where time reversal helps (and may justify its equipment cost).

References

- G.Bal, G. Papanicolaou and L.Ryzhik. *Self-averaging in time reversal for the parabolic wave equation*. Stoch. Dyn., 2 (2002) 507–532
- G.Bal, T.Komorowski and L.Ryzhik, *Self-averaging of Wigner transforms in random media*. Comm. Math. Phys., 242 (2003) 81–135
- G.Bal and L.Ryzhik, *Time Reversal and Refocusing in Random Media*, SIAM J. Appl. Math. 63(5) (2003) 1475-1498
- G.Bal. *On the self-averaging of wave energy in random media*. *Multiscale Model. Simul.*, 2(3), (2004) 398-420, 2004
- G.Bal and R.Verástegui, *Time Reversal in Changing Environment*, Multiscale Model. Simul., 2(4) (2004) 639-661
- G.Bal and O.Pinaud, *Time Reversal Based Detection in Random Media*, Inverse Problems, 21(5) (2005) 1593-1620
- G.Bal and O.Pinaud, *Accuracy of transport models for acoustic waves in random media*, submitted